PHILOSOPHICAL TRANSACTIONS OF THE ROYAL SOCIETY A MATHEMATICAL, PHYSICAL & ENGINEERING SCIENCES

On the Amplitude Dynamics and Crisis in Resonant Motion of Stretched Strings

A. K. Bajaj and J. M. Johnson

Phil. Trans. R. Soc. Lond. A 1992 **338**, 1-41
doi: 10.1098/rsta.1992.0001

On the amplitude dynamics and crisis in resonant motion of stretched strings

By A. K. Bajaj[1] and J. M. Johnson[2]

[1] *School of Mechanical Engineering, Purdue University, West Lafayette, Indiana 47907, U.S.A.*

[2] *Inland Fisher Guide Division, General Motor Corporation, Troy, Michigan 48084, U.S.A.*

Contents

An N-mode truncation of the equations governing the resonantly forced nonlinear motions of a stretched string is studied. The external forcing is restricted to a plane, and is harmonic with the frequency near a linear natural frequency of the string. The method of averaging is used to investigate the weakly nonlinear dynamics. By using the amplitude equations, which are a function of the damping and the frequency of excitation, it is shown that to $O(\hat{\epsilon})$, only the resonantly forced mode has non-zero amplitude. Both planar (i.e. lying in the planar of forcing) and non-planar constant solutions are studied and amplitude–frequency curves are determined. For small enough damping, solutions in the non-planar branch become unstable via a Hopf bifurcation and give rise to a branch of periodic solutions in the amplitude–frequency plane. This branch exhibits several period-doubling bifurcations, but does not

Phil. Trans. R. Soc. Lond. A (1992) **338**, 1–41
Printed in Great Britain

directly result in the formation of a chaotic attractor. At lower values of damping, many other branches of periodic solutions exist. A series of bifurcations leads to the formation of chaotic attractors in some of these solution branches. Various types of interactions between the different solutions are found to result in many interesting phenomena including, the formation of a homoclinic orbit and chaos quenching. These results are discussed in the context of the Sil'nikov mechanism near a homoclinic orbit for a saddle-focus. Results from the investigations of the averaged system are interpreted for the truncated string system using the averaging theory and the theory of integral manifolds. Numerical investigations with the single mode truncation of the non-autonomous string system show that there is a good correspondence even between chaotic solutions of the averaged system and those of the original system.

1. Introduction

Nonlinear vibrations in stretched strings have been the subject of numerous research investigations, the most recent ones being the works of Johnson & Bajaj (1989) and Tufillaro (1989). Following the work of Miles (1984*a*), Johnson & Bajaj (1989) studied the non-planar resonant motions of the string as a function of the excitation frequency, and for sufficiently low damping, were able to predict amplitude-modulated chaotic motions achieved via the process of torus doubling. These quasi-periodic and chaotic motions necessarily arise due to modal interactions between the identical, planar and non-planar, linear vibration modes even though only one spatial mode is externally excited by the periodic forcing. Some of the results in Johnson & Bajaj (1989), specifically, the torus-doubling process and the chaotic amplitude-modulations, have recently been detected in an experiment (Molteno & Tufillaro 1990) where a good qualitative agreement with many of the theoretical results in Johnson & Bajaj (1989) is also reported.

When a string undergoes transverse vibrations, its length must also fluctuate, causing changes in the string tension. The coupling between the transverse and the longitudinal string oscillations is essentially a nonlinear phenomenon and it cannot be captured by linear models. In a linear model, the assumptions of zero longitudinal displacement and small transverse motions lead to the linear wave equation. If both the longitudinal and the transverse displacements are considered small, the simplest model of a stretched string is necessarily nonlinear. This coupling in the nonlinear equations was studied by many authors (Miles 1965; Anand 1966, 1973; Narasimha 1969; Morse & Ingard 1968; Eller 1972) and is sufficient to predict, over a frequency interval, out-of-plane or ballooning motions for the string even when the excitation is restricted to a plane. A detailed description of the general problem of non-planar string vibration and its analysis by the asymptotic technique of multiple timescales can be found in Nayfeh & Mook (1979).

It was pointed out by Miles (1984*a*–*c*) and Maewal (1986, 1987) that the equations describing the amplitude dynamics of the single-mode truncation of a string are similar to those for the weakly nonlinear resonant motions of, a spherical pendulum (Miles 1984*b*), surface waves in a circular cylinder (Miles 1984*c*; Funakoshi & Inoue 1988, 1990), transverse vibrations of an elastic beam (Maewal 1986) and those for an axisymmetric shell (Maewal 1987). The amplitude equations for the different physical systems can be arrived at by varying a single nonlinear parameter and

PHILOSOPHICAL TRANSACTIONS OF THE ROYAL SOCIETY A MATHEMATICAL, PHYSICAL & ENGINEERING SCIENCES

possess identical symmetry properties. In every case, including that of the string, there exist non-planar or mixed-mode solutions over some frequency interval. These non-planar or whirling motions become unstable and bifurcate into quasi-periodic motions via Hopf bifurcation (Iooss & Joseph 1989; Guckenheimer & Holmes 1983). For small enough damping the limit cycle solutions of the amplitude equations can even bifurcate to chaotic solutions (Guckenheimer & Holmes 1983). Some of the more intricate phenomena observed include isolated solution branches, and Rössler and Lorenz type chaotic attractors.

One of the limited number of mechanisms known to be responsible for chaotic behaviour in systems of differential equations is associated with the existence of orbits of infinite period linking one or more saddle points. A trajectory connecting the unstable and stable manifolds of the same saddle point is called a homoclinic orbit; one that connects two different saddle points is called heteroclinic. As a control parameter is increased there may, in certain circumstances, be homoclinic or heteroclinic bifurcations that produce chaotic motions (Guckenheimer & Holmes 1983; Wiggins 1988). In the classic Lorenz system there is a saddle point with real eigenvalues, and an associated symmetrical pair of homoclinic orbits. Bifurcations from this orbit first leads to 'preturbulence' and then to a strange attractor. The other possible case arising in three-dimensional systems corresponds to the equilibrium point being a saddle-focus. Sil'nikov (1970) showed that homoclinic bifurcation in such a system could give rise to chaos. A very insightful and comprehensive study of behaviour near homoclinic orbits in two-parameter systems is the work of Glendinning & Sparrow (1984). More recent extensions to systems with symmetry, and to systems in higher dimensions ($n > 3$) are given in Wiggins (1988) with an excellent summary provided by Mees & Sparrow (1987).

The present work studies the non-planar resonant motions of the string in much more detail than that available in Johnson & Bajaj (1989). The study begins with an N-mode truncation of the partial differential equations and the resonant motions are investigated using the method of averaging. The averaged equations are found to possess very complicated dynamics including isolated and Hopf bifurcating limit cycles branches, various types of chaotic attractors, and the phenomenon of 'boundary crisis' (Grebogi *et al.* 1983). A qualitative discussion of the stable and unstable manifolds along with the computation of chaotic attractors is used to show the occurrence of crisis whereby, at lower damping levels, the chaotic attractors suddenly disappear and do not exist over various excitation frequency intervals. Most of the results predicted by the averaging theory, including the 'crisis', are verified for the truncated string equations. In addition to being comprehensive, the present work includes a careful discussion of the connections between the solutions of the averaged equations and those of the original equations. It is pointed out that some aspects cannot be resolved by the standard results in averaging and the integral manifold theory.

2. Equations of motion and averaging

The equations governing the weakly nonlinear, forced motions of a stretched uniform string were derived by Narasimha (1968) and are given by

$$\boldsymbol{y}_{tt} + 2\delta\omega_1 \boldsymbol{y}_t - \left\{c_0^2 + c_1^2/2l \int_0^1 |\boldsymbol{y}_x|^2 \,\mathrm{d}x\right\} \boldsymbol{y}_{xx} = \frac{1}{m} \boldsymbol{Y}(x,t), \tag{1}$$

where $\boldsymbol{y} \equiv (y, z)^{\mathrm{T}}$ is the lateral displacement of the string at position x, $0 < x < 1$, and at time t. In equation (1), ω_1 is the fundamental frequency of transverse linear vibration of the string; δ is the damping ratio for the fundamental mode, c_0 and c_1 are, respectively, the transverse and the longitudinal wave speeds; l is the length of the string and m is its mass per unit length. $\boldsymbol{Y}$ is the external loading per unit length of the string with the two components Y_1 and Y_2 representing the forces in the y and z directions respectively. The subscripts x and t signify, respectively, partial differentiation with respect to the coordinate x and the time t. These equations were derived, taking into account the longitudinal displacement of the string and its coupling with the transverse motion, along with the change in tension due to the large amplitude of motion. Only the lowest order nonlinear terms were then retained in a successive approximation approach.

Letting

$$\boldsymbol{y}(x,t) = \sum_{n=1}^{\infty} \bar{\boldsymbol{y}}_n(t) \sin\frac{n\pi x}{l}, \quad \boldsymbol{Y}(x,t) = \sum_{n=1}^{\infty} \bar{\boldsymbol{Y}}_n(t) \sin\frac{n\pi x}{l}, \tag{2}$$

and using the orthogonality of the linear modes, equations (1) and (2) yield the modal equations

$$\ddot{\bar{\boldsymbol{y}}}_n + 2\delta\omega_1 \dot{\bar{\boldsymbol{y}}}_n + \omega_n^2 \left\{1 + \frac{1}{4sl_*^2} \sum_{j=1}^{\infty} |j\bar{\boldsymbol{y}}_j|^2\right\} \bar{\boldsymbol{y}}_n = \frac{1}{m} \bar{\boldsymbol{Y}}_n, \quad n = 1, 2, \ldots, \tag{3}$$

where $\omega_n = n\omega_1$ is the natural frequency of the nth linear mode, $s = (c_0/c_1)^2$ is the ratio of the two wave speeds, and $l_* = l/\pi$ is a normalized length.

We now assume that the external forcing is harmonic, its frequency is near the rth natural frequency, ω_r, and it is restricted to, say the xy plane. Then $\bar{\boldsymbol{Y}}_n$ can be written as

$$\bar{\boldsymbol{Y}}_n = \frac{\epsilon m l_* \omega_1^2}{n^{\frac{1}{2}}} \cos\omega t \begin{Bmatrix} \delta_{rn} \\ 0 \end{Bmatrix}, \tag{4}$$

where the scaling has been chosen to simplify subsequent algebraic expressions and δ_{ij} is the Kronecker delta. Note that ϵ represents the amplitude of the harmonic excitation and will be considered 'small'. Also, only the rth spatial mode is excited with the harmonic force. All the other modes, corresponding to $n = 1, 2, \ldots, r-1$, $r+1, \ldots$, are excited only through their nonlinear coupling with the rth mode. In fact, even the out-of-plane component, $\bar{y}_{r2}$, for the rth mode is excited only through its nonlinear coupling with the in-plane component, $\bar{y}_{r1}$.

An N mode truncation of the infinite set of ordinary differential equations (3) can be studied using the asymptotic method of averaging (Hale 1963, 1969) for arbitrary N. To simplify the coefficients of the resulting equations and to explicitly introduce the 'smallness' of motion, the following scaled quantities are defined:

$$z_n = \bar{y}_n \frac{n^{\frac{3}{2}}}{2l_*(\epsilon s)^{\frac{1}{3}}}, \quad \alpha = 4\delta\left(\frac{s}{\epsilon^2}\right)^{\frac{1}{3}}\left(\frac{\omega}{\omega_1 r}\right), \quad \beta = 2r\left(\frac{s}{\epsilon^2}\right)^{\frac{1}{3}}\left[\left(\frac{\omega}{\omega_1 r}\right)^2 - 1\right], \tag{5}$$

$$\tau_1 = (\omega/r)t, \quad \hat{\epsilon} = \tfrac{1}{4}(\epsilon^2/s)^{\frac{1}{3}}.$$

The resulting equations are:

$$z_n'' + n^2 z_n = \hat{\epsilon}\left[2n\cos n\tau_1 \begin{Bmatrix} \delta_{rn} \\ 0 \end{Bmatrix} - 2\alpha z_n' - 2\frac{\beta}{r} z_n'' - 4n^2 \sum_{j=1}^{N} \frac{1}{j} |z_j|^2 z_n\right], \quad n = 1, 2, \ldots, N, \tag{6}$$

where $\mathrm{d}(\cdot)/\mathrm{d}\tau_1 \equiv (\cdot)'$. Equations (6) comprise a system of $2N$ coupled oscillators in

which the planar component of the rth oscillator pair is weakly excited and all the oscillators are weakly coupled through cubic nonlinear terms. The non-dimensional parameters α and β represent, respectively, damping and detuning. The exact resonance condition corresponds to $\beta = 0$. Thus, β represents the deviation of the excitation frequency, ω, from the rth natural frequency, $r\omega_1$.

The scalings defined imply that, in terms of the amplitude of external forcing, ϵ, the displacements, $\bar{y}_n$, are of $O(\epsilon^{\frac{1}{3}})$ whereas the damping, δ, and the frequency detuning, $(\omega^2 - r\omega_1^2)$, are each of $O(\epsilon^{\frac{2}{3}})$. The weakly coupled oscillators in equations (6) have a new small parameter, $\hat{\epsilon}$, which itself is related to the amplitude of the external excitation and will be used as the small parameter in the asymptotic analysis. In terms of $\hat{\epsilon}$, the displacements, damping and detuning (i.e. $\bar{y}_n$, δ and $(\omega^2 - r\omega_1^2)$) are of $O(\hat{\epsilon}^{\frac{1}{2}})$, $O(\hat{\epsilon})$, and $O(\hat{\epsilon})$ respectively.

The weakly nonlinear system (6) is to be investigated using the method of averaging. Let

$$z_n = \hat{\boldsymbol{A}}_n(\tau_1)\cos n\tau_1 + \hat{\boldsymbol{B}}_n(\tau_1)\sin n\tau_1,$$
$$z_n' = -n\hat{\boldsymbol{A}}_n(\tau_1)\sin n\tau_1 + n\hat{\boldsymbol{B}}_n(\tau_1)\cos n\tau_1, \quad n = 1, 2, \ldots, N, \tag{7}$$

where $\hat{\boldsymbol{A}}_n$ and $\hat{\boldsymbol{B}}_n$ are 2-vectors. Substituting equations (7) into equations (6) gives the system in 'standard form'

$$\hat{\boldsymbol{A}}_n' = \hat{\epsilon}\boldsymbol{f}_{1n}(\hat{\boldsymbol{A}}, \hat{\boldsymbol{B}}, \tau_1, \hat{\epsilon}), \quad \hat{\boldsymbol{B}}_n' = \hat{\epsilon}\boldsymbol{f}_{2n}(\hat{\boldsymbol{A}}, \hat{\boldsymbol{B}}, \tau_1 \hat{\epsilon}), \quad n = 1, 2, \ldots, N, \tag{8}$$

where $\boldsymbol{f}_{1n}$ and $\boldsymbol{f}_{2n}$ are bounded 2π-periodic functions of τ_1, and where, notationally, the arguments $\hat{\boldsymbol{A}}$ and $\hat{\boldsymbol{B}}$ signify that the functions $\boldsymbol{f}_{1n}$ and $\boldsymbol{f}_{2n}$ may depend on all the vectors $\hat{\boldsymbol{A}}_1, \ldots, \hat{\boldsymbol{A}}_N$ and $\hat{\boldsymbol{B}}_1, \ldots, \hat{\boldsymbol{B}}_N$. The averaged equations corresponding to the system (8) in 'standard form' are then

$$\boldsymbol{A}_n' = \hat{\epsilon}\boldsymbol{f}_{1n0}(\boldsymbol{A}, \boldsymbol{B}), \quad \boldsymbol{B}_n' = \hat{\epsilon}\boldsymbol{f}_{2n0}(\boldsymbol{A}, \boldsymbol{B}), \quad n = 1, 2, \ldots, N, \tag{9}$$

where $\boldsymbol{f}_{1n0}$ and $\boldsymbol{f}_{2n0}$ are the mean values (averages) of the functions $\boldsymbol{f}_{1n}$ and $\boldsymbol{f}_{2n}$ defined by

$$\boldsymbol{f}_{in0} \equiv \frac{1}{2\pi}\int_0^{2\pi} \boldsymbol{f}_{in}(\boldsymbol{A}, \boldsymbol{B}, \tau_1, 0)\,\mathrm{d}\tau_1, \quad i = 1, 2, \quad n = 1, 2, \ldots, N. \tag{10}$$

The averaged equations (9) depend on the external parameters α and β and provide first-order approximations to the solutions of the original non-autonomous system (8) and, therefore, the truncated string equations (8). The infinite-time theorems in averaging theory and the theory of integral manifolds (Hale 1963, 1969) then relate the steady-state solutions of the averaged system (9) to those of the original system (8). Constant solutions of the averaged system correspond to 2π-periodic solutions of the original system and therefore the coupled oscillators (6) also have 2π-periodic solutions. Periodic solutions of the averaged system correspond to amplitude modulated motions of the coupled oscillators. These relations will be discussed in much more detail in §5.

After averaging, the equations for $\boldsymbol{A}_n$ and $\boldsymbol{B}_n$ are explicitly given by

$$\boldsymbol{A}_n' = \hat{\epsilon}\left[-\alpha\boldsymbol{A}_n - \frac{n}{r}\beta\boldsymbol{B}_n + n\sum_{j=1}^{N}\frac{1}{j}E_j\boldsymbol{B}_n - \tfrac{1}{2}(|\boldsymbol{A}_n|^2 - |\boldsymbol{B}_n|^2)\boldsymbol{B}_n + (\boldsymbol{A}_n\cdot\boldsymbol{B}_n)\boldsymbol{A}_n\right], \tag{11}$$

$$\boldsymbol{B}_n' = \hat{\epsilon}\left[\begin{Bmatrix}\delta_{rn}\\ 0\end{Bmatrix} - \alpha\boldsymbol{B}_n + \frac{n}{r}\beta\boldsymbol{A}_n - n\sum_{j=1}^{N}\frac{1}{j}E_j\boldsymbol{A}_n - \tfrac{1}{2}(|\boldsymbol{A}_n|^2 - |\boldsymbol{B}_n|^2)\boldsymbol{A}_n - (\boldsymbol{A}_n\cdot\boldsymbol{B}_n)\boldsymbol{B}_n\right],$$
$$n = 1, 2, \ldots, N,$$

where $E_n \equiv (\boldsymbol{A}_n\cdot\boldsymbol{A}_n) + (\boldsymbol{B}_n\cdot\boldsymbol{B}_n)$ and $(\boldsymbol{u}\cdot\boldsymbol{v})$ is the usual vector dot product.

In the truncated string system (6), the planar and the non-planar components for each spatial mode (z_{r1} and z_{r2} respectively) have identical frequencies (1:1 internal resonance). Furthermore, the linear natural frequencies for the various spatial modes are all multiples of the lowest natural frequency. Thus, numerous internal resonances (Nayfeh & Mook 1979) of the type $p:(p+q)$, $p, q = 1, 2, 3, \ldots$, are present in the string system. However, the response of the indirectly excited modes remains small in this case because equations (6) do not possess the proper type of nonlinear coupling terms. To see that only the mode in external resonance (which includes both the in-plane component and its out-of-plane counterpart due to the 1:1 internal resonance) may possess a large steady-state response, consider the rate of change $\mathrm{d}E_n/\mathrm{d}\tau_1$ of E_n. By using the definition of E_n and equations (11), it is easy to show that

$$\frac{1}{2}\frac{\mathrm{d}E_n}{\mathrm{d}\tau_1} = \hat{\epsilon}\left[-\alpha E_n + \left(\begin{Bmatrix}\delta_{rn}\\ 0\end{Bmatrix}\boldsymbol{B}_n\right)\right]. \tag{12}$$

Clearly, for $n \neq r$ and to $O(\hat{\epsilon})$, the energy, E_n, exponentially decays to zero as $\tau_1 \to \infty$. Thus, for the unforced modes, the only steady-state solution possible is the trivial solution. Also note that, for $n = r$ and to $O(\hat{\epsilon})$, the energy, E_r, is decoupled from all other modes. Therefore the trajectories of the $4N$-dimensional system defined by equations (11) quickly collapse to the four-dimensional subspace associated with just the resonantly forced mode. In other words, the long term dynamics of the averaged equations governing the resonantly forced mode play a pivotal role in determining the long term dynamics of the larger system. Letting $\boldsymbol{p} = (p_1, p_2)^{\mathrm{T}} = \boldsymbol{A}_r$, and $\boldsymbol{q} = (q_1, q_2)^{\mathrm{T}} = \boldsymbol{B}_r$, the reduced equations (11), governing the dynamic behaviour of the resonantly forced mode turn out to be

$$\left.\begin{aligned} \dot{p}_1 &= -\alpha p_1 - (\beta - 1.5E)q_1 + Mp_2, \quad \dot{q}_1 = -\alpha q_1 + (\beta - 1.5E)p_1 + Mq_2 + 1,\\ \dot{p}_2 &= -\alpha p_2 - (\beta - 1.5E)q_2 - Mp_1, \quad \dot{q}_2 = -\alpha q_2 + (\beta - 1.5E)p_2 - Mq_1, \end{aligned}\right\} \tag{13}$$

where $E = E_r$, $M = p_1 q_2 - p_2 q_1$, and where a dot now represents derivative with respect to the slow timescale $\tau \equiv \hat{\epsilon}\tau_1$. These equations are independent of the mode which is being resonantly forced. Therefore, without loss of generality, it can be assumed that $r = 1$. Note that the mode number, r, does appear explicitly in the scalings defined in (5).

It is important to note here that the system (13) is quasi-hamiltonian. The divergence of the system in the four-dimensional phase space,

$$\sum_{i=1}^{2}\frac{\partial \dot{p}_i}{\partial p_i} + \frac{\partial \dot{q}_i}{\partial q_i},$$

is -4α from which it follows that every trajectory must ultimately be confined to a limiting subspace of dimension less than four. Furthermore, the system is invariant to the transformation $(p_2, q_2) \to (-p_2, -q_2)$. Thus, the equations (13) have pairwise steady-state solutions unless the solution in question itself satisfies this symmetry.

As was mentioned in the Introduction, the amplitude equations (13) are a special case of a one-parameter family of equations of the form

$$\left.\begin{aligned} \dot{p}_1 &= -\alpha p_1 - (\beta + \tfrac{1}{2}AE)q_1 + BMp_2, \quad \dot{q}_1 = -\alpha q_1 + (\beta + \tfrac{1}{2}AE)p_1 + BMq_2 + 1,\\ \dot{p}_2 &= -\alpha p_2 - (\beta + \tfrac{1}{2}AE)q_2 - BMp_1, \quad \dot{q}_2 = -\alpha q_2 + (\beta + \tfrac{1}{2}AE)p_2 - BMq_1. \end{aligned}\right\} \tag{14}$$

The string equations are obtained by letting $A = -3$ and $B = 1$. The various systems

studied by Miles (1984*b*, *c*) and Maewal (1986, 1987) can be obtained by varying A and B. Maewal's beam equations correspond to $-B/A = 1.71$ whereas Miles's equations governing a spherical pendulum correspond to $-B/A = 3$. In both Maewal's work on axisymmetric shells and Miles's work (also Funakoshi & Inoue 1988, 1990) on surface waves in a circular cylinder, the ratio $-B/A$ can be varied by changing some relevant physical parameters.

3. Constant solutions of the averaged equations

The constant solutions of the averaged equations (14) have been studied extensively by Miles (1984*c*). These results were specialized for the string problem in Miles (1984*a*) and in Johnson & Bajaj (1989). Some of the results are again repeated here for their relevance and, for completeness of the discussion. The stability of the constant solutions is determined using the eigenvalues of the jacobian matrix. Additionally, some qualitative discussion of the stable and unstable manifolds of the fixed points is undertaken as it will provide very useful information about the dynamic behaviour, including the phenomenon of 'crisis'.

The constant solutions $(p_1, q_1, p_2, q_2)^{\mathrm{T}}$ of the equations (14) need to be determined as a function of the detuning, β, and the damping, α. These equations can be solved easily (Miles 1984*c*) to get the state variables $p_i, q_i, i = 1, 2$ in terms of the combinations $E \equiv p_1^2 + q_1^2 + p_2^2 + q_2^2$ and $M \equiv p_1 q_2 - p_2 q_1$. The functions M and E themselves satisfy the following two sets of polynomials:

$$M = 0,\ A^2E^3 + 4\beta AE^2 + 4(\beta^2 + \alpha^2)E - 4 = 0, \tag{15}$$

and

$$B^2M^2 = -\tfrac{1}{4}A(A+2B)E^2 - \beta(A+B) - (\beta^2+\alpha^2),$$

$$2A(A+B)^2E^3 + 4\beta(3A+B)(A+B)E^2 + 8\{\alpha^2 A + (3A+2B)\beta^2\}E + \{4B + 16\beta(\alpha^2+\beta^2)\} = 0. \tag{16}$$

The solutions of equations (15) and (16) can be studied as a function of the parameters β and α. Only those roots for which E is real and positive, and $M^2 \geqslant 0$ are physically meaningful.

Equations (15) and (16) implicitly define the frequency-response curves in the βE plane (for fixed α). Solutions of equations (15) require that $M = 0$, which is possible only when $p_2 = q_2 = 0$. Clearly, such a solution remains in the plane of excitation and will be, henceforth, called the planar branch. In general, solutions of equations (16) will have $M \neq 0$ which implies that the p_2 and q_2 are non-zero, and such solutions will be referred to as the non-planar branch. Notice that, because of symmetry, the pairs (E, M) and $(E, -M)$, simultaneously, satisfy equations (16). Thus, there are in fact two symmetric pairs of non-planar branches given by (p_1, q_1, p_2, q_2) and $(p_1, q_1, -p_2, -q_2)$.

Miles (1984*c*) has discussed the solutions of (15) and (16) as a function of the frequency detuning β and the damping α. This analysis includes a careful study of turning points, number of meaningful solutions, maximum values as well as the static and Hopf bifurcation sets in the $\alpha\beta$ plane. Miles, additionally, obtained approximations for these sets using asymptotic expansions in the damping parameter, α. These results have been further elaborated and extended in Johnson (1989). In the following paragraphs, we only present numerical results for the case of the string system which corresponds to the nonlinear coefficients being $A = -3.0$, $B = 1.0$.

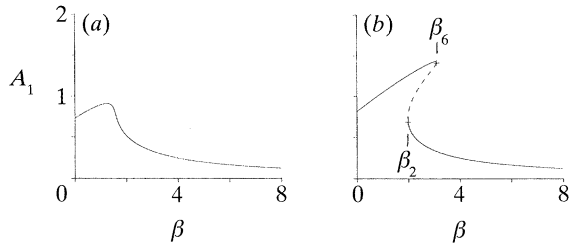

Figure 1. Constant amplitude response curves for the string: (*a*) $\alpha = 1.1$; (*b*) $\alpha = 0.7$.

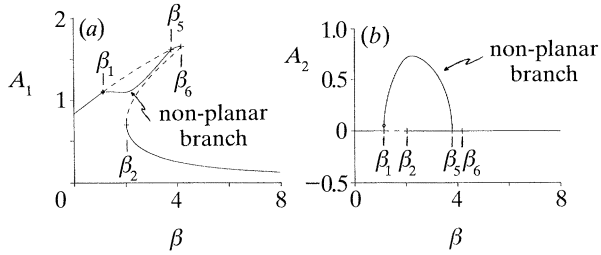

Figure 2. Constant amplitude response curves for the string: $\alpha = 0.6$.

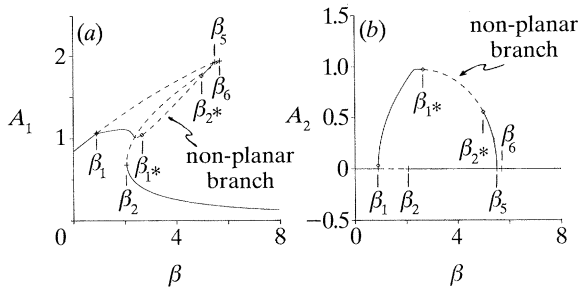

Figure 3. Constant amplitude response curves for the string; $\alpha = 0.513$.

(*a*) *Response curves for the string*

In figures 1–4, the response curves for the string are plotted for several representative values of damping. The figures show the planar amplitude, $A_1 \equiv p_1^2 + q_1^2$, and the non-planar amplitude, $A_2 \equiv p_2^2 + q_2^2$, as a function of β for fixed α.

Analysis in Miles (1984*c*) and Johnson (1989) shows that for large damping values ($\alpha > 0.991$), only the planar branch exists and that it is single valued for all β. Figure 1*a* is typical of the response curves of this type. The string, therefore, has a unique steady-state periodic response at each frequency of excitation. This response remains in the plane of excitation. For $\alpha < 0.991$ the planar branch is multi-valued in the interval (β_2, β_6). Figure 1*b* is typical of the response curves of this type. Here again, the motion of the string is confined to the plane of excitation except that in the frequency interval (β_2, β_6) three steady-state solutions are possible. As α is decreased the planar solution branch undergoes a pitchfork bifurcation and gives rise to two symmetric non-planar solution branches.

The non-planar branch is known (Miles 1984*c*; Johnson 1989) to exist provided $\alpha < 0.687$. In fact, there are two non-planar solution branches due to symmetry, but from here forward they will be referred to collectively as the non-planar branch. For large enough damping values ($\alpha > 0.477$), the non-planar branch is single valued.

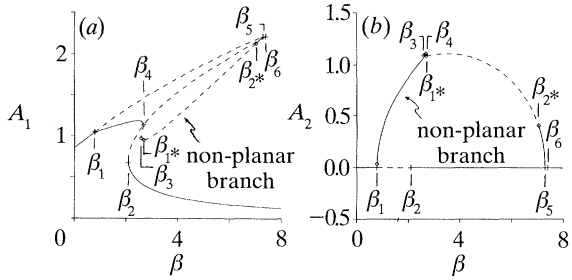

Figure 4. Constant amplitude response curves for the string; $\alpha = 0.45$.

Figures 2 and 3 are typical of the response curves of this type. For $\alpha < 0.477$, the non-planar branch is multi-valued in the interval (β_3, β_4). Figure 4 shows a typical response curve of this type. It is clear from these curves that for some frequencies stable non-planar solutions of the string coexist with planar solutions. In figures 1–4, stable solutions are shown in solid lines, whereas unstable solutions are shown in dashed lines. We now discuss the stability of the planar and the non-planar fixed points.

Let the characteristic equation for the jacobian matrix of equations (13) around a steady-state constant solution be

$$J_4\lambda^4 + J_3\lambda^3 + J_2\lambda^4 + J_1\lambda + J_0 = 0, \tag{17}$$

where J_i, $i = 0, \ldots, 4$ depend on the solution and the parameters α and β. Sethna & Bajaj (1978) showed that for fourth-order quasi-hamiltonian systems, there are two ways in which a stable equilibrium point may become unstable as some system parameter is varied. Either an eigenvalue must pass through the origin or a complex conjugate pair of eigenvalues must pass through the imaginary axis with non-zero imaginary parts. They further showed that the first type of instability occurs when

$$J_0 = \mathrm{Det}\,[\partial \boldsymbol{f}/\partial \boldsymbol{x}] = 0, \tag{18}$$

and that the second type of instability occurs when

$$J_1(J_2J_3 - J_1J_4) - J_0J_3^3 = 0. \tag{19}$$

In the response curves shown in the figures 1–4, both types of instabilities arise. The first type of instability arises at the critical points, $\beta_i, j = 1, \ldots, 6$. The points β_2, β_6 and β_3, β_4 correspond to turning points in the planar and non-planar solution branches, respectively. At points β_1, and β_5 there is a pitchfork type bifurcation from planar solutions to non-planar solutions and the two solutions undergo an exchange in sign of one real eigenvalue.

The second type of instability, defined by condition (19), (obtained using Routh–Hurwitz criterion) is the well-known Hopf bifurcation. The non-planar fixed point undergoes a Hopf bifurcation. These bifurcation points are labelled β_{1*} and β_{2*} in figures 3 and 4. The points β_{1*} and β_{2*} only exist provided that the damping is below a critical value ($\alpha = 0.577$ for the string problem). From the Hopf bifurcation theorem (Iooss & Joseph 1989; Guckenheimer & Holmes 1983), it is expected that for the averaged equations (13) a limit cycle arises near β_{1*} and β_{2*}. Figure 5 shows the Hopf bifurcation set in the $\alpha\beta$ plane. It is clear from this figure that β_{1*} and β_{2*} coalesce as the damping α is increased.

The importance of the Hopf bifurcation theorem to the study of nonlinear systems is difficult to overstate. Hopf bifurcations provide a means by which relatively

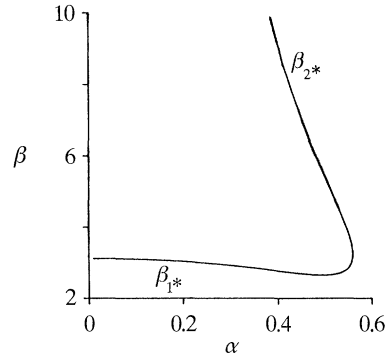

Figure 5. Hopf bifurcation set in the $\alpha\beta$ plane.

mundane constant solutions give rise to more complicated time dependent steady-state solutions. This is important to the study of nonlinear dynamical systems because there is currently no way of, *a priori*, knowing of the existence of complex solutions in a particular system for a particular set of parameter values. Furthermore, even if complex solutions are suspected, it is not known where in the phase space these interesting solutions exist. The Hopf bifurcation theorem, where applicable, provides insight into the parameter range in which interesting solutions can be found and also indicates the location in the phase space of such limit cycle or periodic solutions.

The study of the averaged equations, thus far, has shown that for large damping values the only constant solutions that exist are in the plane of the external forcing. The response is like that of Duffing's equation near primary resonance (Nayfeh & Mook 1979) with multiple solutions arising between the frequencies β_2 and β_6. Though the model includes out-of-plane motions, all the out-of-plane disturbances decay exponentially to zero. Further reduction in damping destabilizes the upper planar branch to out-of-plane disturbances, resulting in non-planar or whirling motions of the string in the frequency interval (β_1, β_5). Now it is possible to generate planar as well as non-planar steady-state periodic responses by simply adjusting the initial conditions. In fact, it was shown in Johnson & Bajaj (1989) that the non-planar branch itself develops multiple constant solutions as well as Hopf bifurcation which lead to stable limit cycle solutions coexisting with planar and non-planar constant solutions.

The following section discusses the stable and the unstable manifolds of the fixed points as they play an important role in the global dynamical behaviour of the nonlinear system.

(*b*) *Stable and unstable manifolds of equilibrium points*

The stable manifold of a fixed point is the set of all initial conditions such that the solution of the differential equation started at these points leads asymptotically to the fixed point as $t \to +\infty$. The unstable manifold of a fixed point is similarly defined for $t \to -\infty$. These stable and unstable manifolds of equilibrium points provide important information about the transient behaviour of a dynamical system. The manifolds of saddle-type equilibrium points determine the domains of attraction of the stable steady-state solutions or attractors of the system. The dimension of the stable manifold of an equilibrium point equals the number of eigenvalues of the jacobian that are in the left-half plane. Furthermore, the stable manifold is tangent

Figure 6

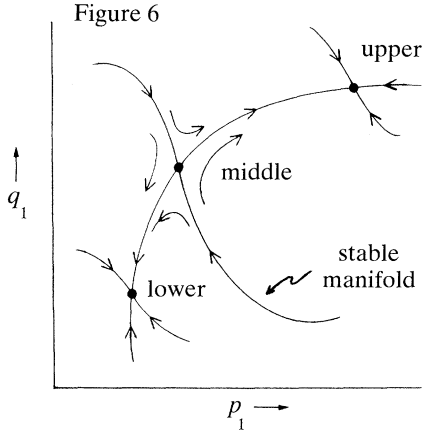

Figure 7

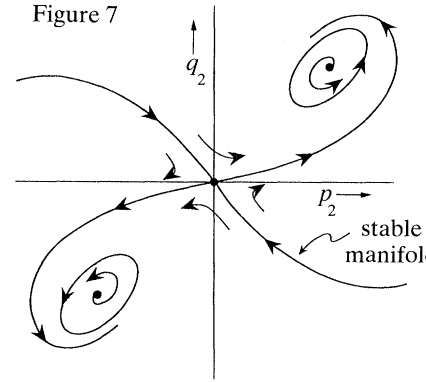

Figure 6. Planar flow field for the averaged system.

Figure 7. Flow field near Hopf bifurcation from non-planar solutions.

to the linear subspace generated by the stable eigenvectors of the fixed point. Similar statements can be made concerning the unstable manifold. A complete discussion of stable and unstable manifolds can be found in Wiggins (1988).

In the averaged equations being studied here, many equilibrium points arise as the parameters α and β are varied. These solutions, furthermore, undergo stability changes. Thus, there are several important manifolds to discuss. For ease of discussion, it is convenient to begin with the case of large damping so that only the planar constant solutions exist. In parameter regions where more than one equilibrium point exists, they will be referred to as the lower, the middle and the upper planar fixed point.

Consider the invariant manifolds associated with the middle planar fixed point. Since this fixed point has one eigenvalue in the right-half plane, the unstable manifold is one dimensional. As a consequence of the fact that the middle solution branch terminates at both ends via saddle-node bifurcations (i.e. turning points), the unstable manifold of the middle fixed point must lead to the upper fixed point in one direction and the lower fixed point in the other. The stable manifold of the middle planar fixed point forms a three-dimensional hyper-surface that, in a sense, partitions the phase space. Solutions beginning on one side must remain on that side for all time (both positive and negative times). Furthermore, all the initial conditions on one side asymptotically lead to the same stable fixed point as $t \to +\infty$. Thus, the stable manifold of the middle fixed point defines the domains of attraction of the lower and upper planar fixed points. This can be more easily seen by considering the flow field in the $p_1 q_1$ plane. Note that the $(p_1 q_1)$ sub-manifold itself is asymptotically stable and is an invariant of the system. Figure 6 qualitatively shows a typical flow field for a frequency, β, where only the three planar fixed points exist. As β is increased to β_6 (the right planar turning point), the middle and the upper planar fixed points coalesce. As β is decreased to β_2 (the left planar turning point), the middle and the lower planar fixed points coalesce.

The manifolds of the upper planar fixed point assume importance for values of damping for which the fixed point is unstable (i.e. when the non-planar branch exists). In this case, the stable and the unstable manifolds are very similar to those of the middle planar fixed point. The stable manifold partitions the space into

PHILOSOPHICAL TRANSACTIONS OF THE ROYAL SOCIETY A MATHEMATICAL, PHYSICAL & ENGINEERING SCIENCES

symmetric domains of attraction for the two non-planar fixed points. The unstable manifolds lead to the two non-planar fixed points (at least when the non-planar fixed points are stable).

When the non-planar equilibrium points become unstable via a Hopf bifurcation, the unstable manifolds of the upper planar constant solution no longer lead to the non-planar fixed points, rather, they asymptotically approach the more interesting non-planar solutions such as limit cycles. Figure 7 qualitatively shows the vector field projected onto the $p_2 q_2$ plane. Since the stable manifold of the middle planar constant solution separates the upper and the lower planar fixed points, the unstable manifold of the upper planar fixed point cannot lead to the stable lower planar fixed point.

The unstable manifold of the upper planar equilibrium point, in parameter regions where the non-planar fixed points are unstable, is extremely important to the investigation of non-constant solutions of the averaged equations (13). This unstable manifold leads neither to a stable fixed point nor to infinity (the asymptotic solutions set is bounded). Several authors have noted that chaotic attractors seem to be a subset of the closure of the unstable manifold of a saddle-type fixed point (Grebogi *et al.* 1983). This observation provides a very powerful and useful means of finding initial conditions that lead to interesting solutions of the averaged equations (e.g. limit cycles and chaotic attractors).

The following section makes use of the understanding gained here in an exhaustive numerical investigation of the averaged equations (13). In particular, knowledge of the existence of Hopf bifurcation in the non-planar branch, coupled with the knowledge of the planar and non-planar constant solutions and the corresponding invariant manifolds provides a solid base from which to study the averaged equations (13) for more interesting steady-state behaviour such as limit cycles and chaotic attractors.

4. Periodic and chaotic solutions of averaged equations

In this section the averaged equations (13) are studied for periodic and chaotic solutions using numerical techniques. As is already shown by Johnson & Bajaj (1989), the Hopf bifurcation discussed in the previous section gives rise to a stable limit cycle. Apart from the Hopf branch, many other branches of periodic solutions are discovered and investigated. These periodic solution branches exhibit many interesting phenomena including saddle-node bifurcations, period-doubling bifurcations and the formation of a homoclinic orbit. In some branches, a cascade of period-doubling bifurcations results in the formation of a chaotic attractor. These attractors are characterized using Poincaré sections, Lyapunov exponents, and the concept of fractal dimension. The chaotic attractor grows quickly in size as damping is reduced, so much so that it collides with its basin boundary and is destroyed through a process termed 'crisis'. As many of these results are well documented in Johnson & Bajaj (1989) we present the results selectively, concentrating on the new and much more interesting aspects of the dynamical behaviour.

(*a*) *Non-existence of planar periodic solutions*

Consider the averaged equations (14) for the family of systems. It was shown in the last section that $p_2 = q_2 = 0$ is an invariant manifold and on this submanifold the dynamical behaviour is determined by the two first-order differential equations

PHILOSOPHICAL TRANSACTIONS OF THE ROYAL SOCIETY A MATHEMATICAL, PHYSICAL & ENGINEERING SCIENCES

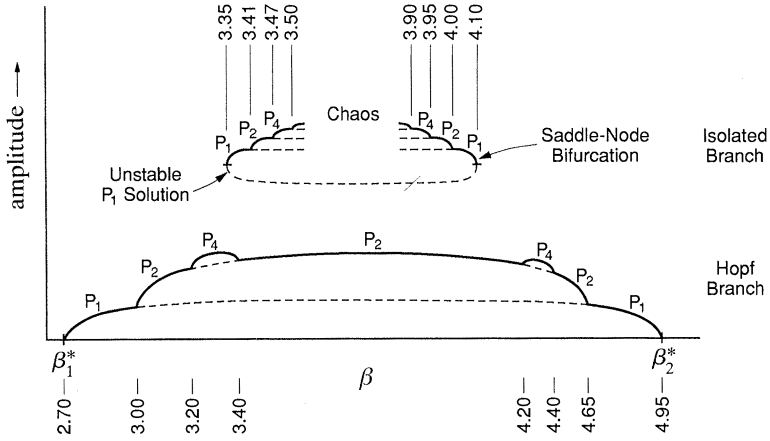

Figure 8. Approximate bifurcation points in the periodic solution branches and the bifurcation diagrams; $\alpha = 0.513$.

governing the variables p_1 and q_1. The divergence of the vector field restricted to the $p_2 = q_2 = 0$ submanifold, $\partial\dot{p}_1/\partial p_1 + \partial\dot{q}_1/\partial q_1$, is -2α which is always of the same sign. Thus, for the planar system, Bendixon's criterion (Guckenheimer & Holmes 1983) is satisfied and limit cycles are ruled out. If there are periodic solutions for the averaged equations, they only arise in the complete four-dimensional system.

(*b*) *The Hopf solution branch*

For $\alpha > 0.577$, the non-planar constant solutions of the averaged equations are stable. The only unstable constant solutions are the planar solutions and these arise due to steady bifurcations. However, for $\alpha < 0.577$, a portion of the non-planar branch becomes unstable by Hopf bifurcation. The Hopf bifurcation is supercritical and a stable limit cycle is created near the fixed point for parameter values for which the fixed point is unstable. For damping near 0.577, the limit cycle is stable over the entire detuning interval (β_{1*}, β_{2*}). It grows from zero amplitude at β_{1*} to some finite size and then shrinks back to the fixed point at β_{2*}. Thus, there is a single connected periodic branch joining points β_{1*} and β_{2*}. Since the non-planar solutions exist in symmetric pairs, there is another stable limit cycle. The existence of the symmetric pair of solutions will be explicitly mentioned only when necessary.

Reduction in damping results in the limit cycles in the Hopf solution branch undergoing a period-doubling bifurcation. Many period-doublings can arise depending on the value of α. For $\alpha = 0.513$ the approximate bifurcation points and the type of solutions found in the various frequency intervals are indicated in figure 8. It is clear that the bifurcation structure is quite rich, although no chaotic motions arise in the Hopf branch.

(*c*) *The isolated solution branch*

While numerically investigating the Hopf solution branch, a new and different branch of periodic solutions was discovered. Note that the method used to generate dynamic solutions was simply the long time integration of the differential equations, starting with initial conditions close to the unstable non-planar constant solution. Clearly, long time integration cannot generate unstable solutions. However, several observations led to the following conjectures. This new branch is not connected to the Hopf branch and corresponds to a limit cycle as the primary solution. It arises

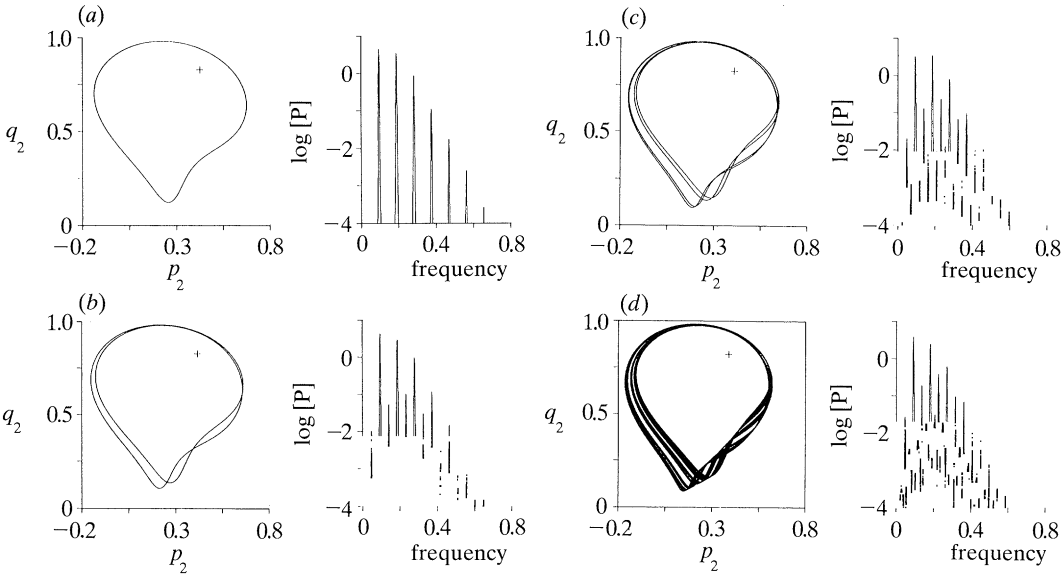

Figure 9. Phase plots and frequency spectra of solutions in the isolated solution branch; $\alpha = 0.513$. (*a*) P_1 solution, $\beta = 3.40$; (*b*) P_2 solution, $\beta = 3.45$; (*c*) P_4 solution, $\beta = 3.50$; (*d*) chaos, $\beta = 3.60$.

due to a global saddle-node bifurcation; that is, a stable and an unstable limit cycle arise at some low enough damping and the branch exists over a small interval in the detuning, β. One indication that this branch is different from the Hopf branch is that the shapes of the solutions on the two branches have distinct characteristics. Also, the newly discovered branch disappears abruptly as the frequency is varied, indicative of the type of jump phenomenon that is associated with saddle-node bifurcations. Finally, the Hopf branch is complete and all its branchings are accounted for, as shown in figure 8. The conjectures concerning the isolated branch have since been verified using AUTO (Doedel 1986). As the damping, α, is decreased, this isolated branch of periodic solutions undergoes a sequence of period-doubling bifurcations which ultimately leads to the formation of a chaotic attractor. Figure 9 gives a representative set of phase plots along with the spectra for solutions in the isolated branch for $\alpha = 0.513$ and for several values of the detuning, β. This chaotic attractor is a 'Rössler' type attractor, that is, it encircles only one unstable fixed point.

The approximate bifurcation points in the isolated branch, and its relation with the Hopf branch, are shown in figure 8. At this level of damping, the isolated branch is created at $\beta \approx 3.35$, goes through a sequence of bifurcations, and ultimately terminates at $\beta \approx 4.10$, again, via a saddle-node bifurcation. It is clear from figure 8 that chaotic solutions of the averaged system coexist with other simpler steady-state stable solutions and that relatively close initial conditions can lead to three very different steady-state solutions (Johnson & Bajaj 1989).

In addition to phase plane plots and frequency spectra, there are other methods of characterizing various attractors or steady-state solutions. These include Poincaré sections, Lyapunov exponents (Benettin *et al.* 1980; Wolf *et al.* 1985) and the various concepts of a dimension (Farmer *et al.* 1983; Parker & Chua 1987). Figure 10 gives the projection onto the $p_2 q_2$ plane of the Poincaré section for the Rössler type attractor at $\alpha = 0.513$, $\beta = 3.6$. The surface of section is the hyperplane $p_1 = 0$ (only

PHILOSOPHICAL TRANSACTIONS OF THE ROYAL SOCIETY A MATHEMATICAL, PHYSICAL & ENGINEERING SCIENCES

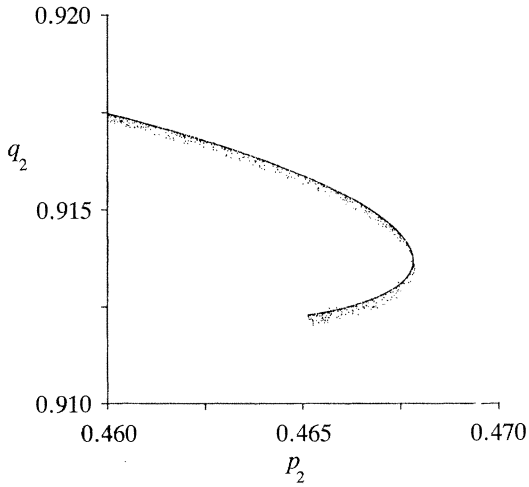

Figure 10. Poincaré section of the Rössler type chaotic attractor; $\alpha = 0.513$, $\beta = 3.6$.

trajectories that pass through the hyperplane $p_1 = 0$ with $\dot{p}_1 > 0$ are included in the figure).

Lyapunov exponents (Benettin *et al.* 1980; Wolf *et al.* 1985) are a measure of the mean exponential convergence (or divergence) of nearby trajectories and can be thought of as generalizations of the eigenvalues associated with fixed points and the Floquet exponents associated with periodic solutions. In the present work, the algorithm of Benettin *et al.* (1980) was used to calculate all the Lyapunov exponents. The Lyapunov exponents for the Rössler type chaotic attractor shown in figure 10 are found to be (0.019, 0.000, −1.025, −1.046).

Another means of characterizing a chaotic attractor is through the concept of dimension (Farmer *et al.* 1983). There are several generalizations of the idea of dimension that help to classify fractal sets, while yielding the expected result for simple sets with integer dimension. Included among these are the capacity dimension, the information dimension, the correlation dimension, and the Lyapunov dimension. For sets defined by dynamical systems, the following dimension based on Lyapunov exponents, has been proposed by Kaplan & Yorke (Kaplan & Yorke 1978; Frederickson *et al.* 1983). Order the Lyapunov exponents of the trajectory such that $\lambda_1 \geqslant \ldots \geqslant \lambda_n$, then the Lyapunov dimension, D_{L}, of the corresponding set is defined as

$$D_{\mathrm{L}} = j + (\lambda_1 + \ldots + \lambda_j)/|\lambda_{j+1}|, \tag{20}$$

where j is chosen such that $\lambda_1 + \ldots + \lambda_j > 0$ but $\lambda_1 + \ldots + \lambda_{j+1} < 0$. In terms of the Lyapunov exponents, j is the 'expansion' dimension of the dynamics, i.e. there are volumes of this dimension which expand. By using the definition (20) and the exponents already calculated, the chaotic attractor shown in figure 10 is found to have $D_{\mathrm{L}} = 2.018$. This implies that a minimum of three state variables are needed to capture the dynamics of the system for these values of parameters.

(*d*) *Isolated branch cascade*

As discussed in the previous section, an isolated branch is created by a saddle-node bifurcation as α is reduced. The fact that the isolated branch involves unstable limit cycles makes it difficult to study this branch using long time integration. In recent years sophisticated algorithms have been developed for numerical bifurcation

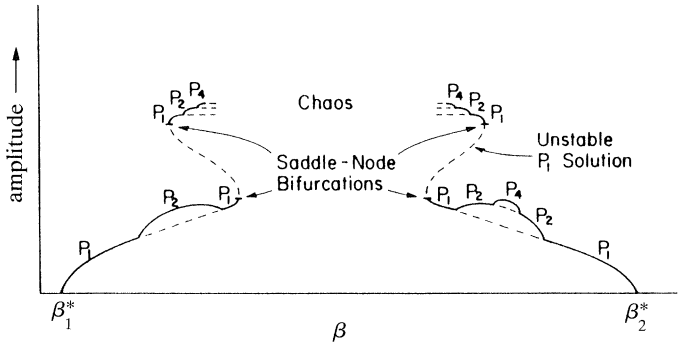

Figure 11. Qualitative bifurcation diagram; $\alpha = 0.50$.

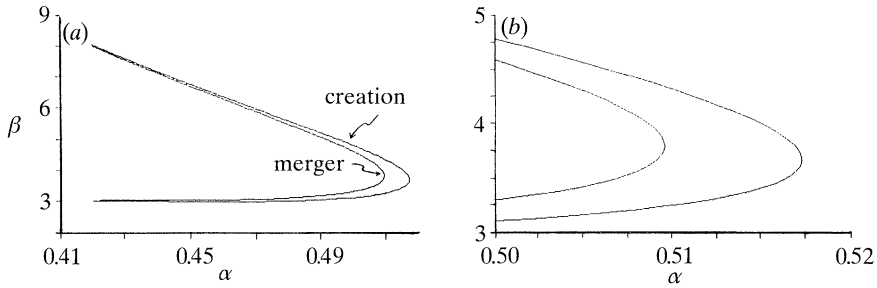

Figure 12. Saddle-node bifurcation sets for the first isolated periodic solutions branch in the $\alpha\beta$ plane.

analysis of ordinary differential equations. AUTO (Doedel 1986) is one of the powerful packages available for bifurcation analysis and continuation of solutions, and it proved to be an invaluable tool in the numerical investigations in this work. AUTO is able to compute solution branches for both constant and periodic solutions. In addition, it can help construct 'saddle-node' and 'Hopf' bifurcation sets in two parameter space. Not only did it allow the conjectures of §4*b* concerning the nature of the isolated branch to be verified, it also made possible the discovery of other unexpected and interesting phenomena.

Returning to the discussion of the isolated branch, we conjectured that, as α is reduced, an isolated periodic solutions branch is created by a saddle-node bifurcation. For even lower values of damping, it was discovered that the Hopf branch ceases to exist in a small interval of the frequency detuning β. This led to the conjecture that the unstable limit cycle associated with the isolated branch has merged, via a saddle-node bifurcation, with the stable limit cycle of the Hopf branch. This merger results in the creation of a frequency interval where the Hopf branch does not exist. From another perspective, as α is increased from a low level, the isolated branch pinches off from the Hopf branch. It is convenient to continue to refer to this branch as the 'isolated branch' even though it is not truly isolated at low damping values. Figure 11 qualitatively shows the sequence of bifurcations in regions where the isolated branch has merged with the Hopf branch. The conjectures made using clues obtained through long time integration, were verified using AUTO. Figure 12 shows a partial saddle-node bifurcation set for the isolated solutions in the $\alpha\beta$ plane where the saddle-node bifurcations occur. The curve marked 'creation' corresponds to the saddle-node bifurcation that creates the isolated branch. The curve marked 'merger'

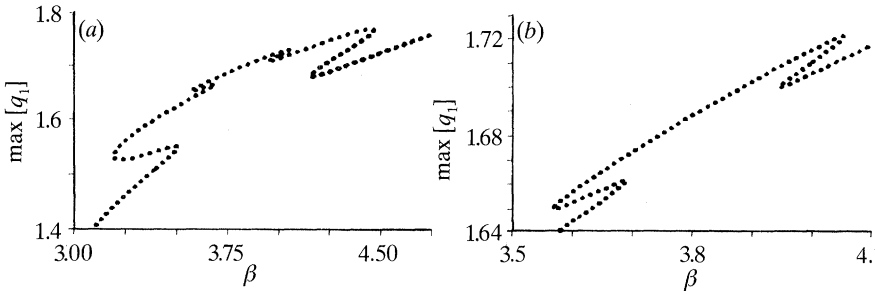

Figure 13. Maximum value of q_1 for P_1 solutions; $\alpha = 0.507$.

corresponds to the saddle-node bifurcation that merges the isolated branch with the Hopf branch. Thus, the first isolated limit cycles branch exists for damping values in the interval *ca.* (0.510–0.518).

By using AUTO and investigating further, it is found that at even lower values of damping, a second isolated branch is created and then merged with the first isolated branch in exactly the same manner that the first isolated branch is created and merged with the Hopf branch. Figure 13 shows, for $\alpha = 0.507$, the P_1 solution branch emanating from the Hopf bifurcation points. Notice that there are now two sets of turning points in this branch. The first pair corresponds to the creation and merger of the first isolated branch. The second pair corresponds to the creation and merger of a second isolated branch. Figure 14 gives the saddle-node bifurcation set corresponding to this second isolated periodic solutions branch along with the already shown (figure 13) saddle-node bifurcation points for the first isolated branch. Notice that there is a range of damping values for which the second isolated branch is truly isolated, meaning that it has pinched off from the first isolated branch.

The process of creation and merger seems to have a stabilizing effect on the previously existing branch. Notice that the Hopf branch does not period-double to infinity in a straightforward manner. It begins to period-double but, in a sense, is constrained by the first isolated branch. The period-doublings are reversed by the presence of the unstable P_1 solution associated with the first isolated branch. The Hopf branch must reverse period-double all the way back to a P_1 solution so that it can merge with the unstable P_1 branch. Similarly, the second isolated branch forces the Rössler type chaos arising from the first isolated branch to reverse bifurcate back to a P_1 solution so that it can merge with the unstable P_1 branch associated with the second isolated branch.

As α is decreased, a cascade of isolated branch creations and mergers occurs. Each new isolated branch has a period longer than that of the previous one. This cascade ultimately leads to the formation of a homoclinic orbit, a trajectory that asymptotically approaches a saddle-type fixed point as $t \to +\infty$ and as $t \to -\infty$. Figure 14 shows a plot of the period of the P_1 solution, T, as a function of the frequency detuning β for a damping value for which the homoclinic orbit exists. This figure clearly shows T approaching a vertical asymptote as the cascade ensues.

(*e*) *Homoclinic orbit and Sil'nikov mechanisms*

The very interesting, though complex, sequence of bifurcations and behaviour described here for the string, were apparently first observed by Knobloch & Weiss (1983) in a fifth-order model of magnetoconvection. Their system possessed reflection symmetry very much like the averaged equations (13) being studied here. Their

PHILOSOPHICAL TRANSACTIONS OF THE ROYAL SOCIETY A MATHEMATICAL, PHYSICAL & ENGINEERING SCIENCES

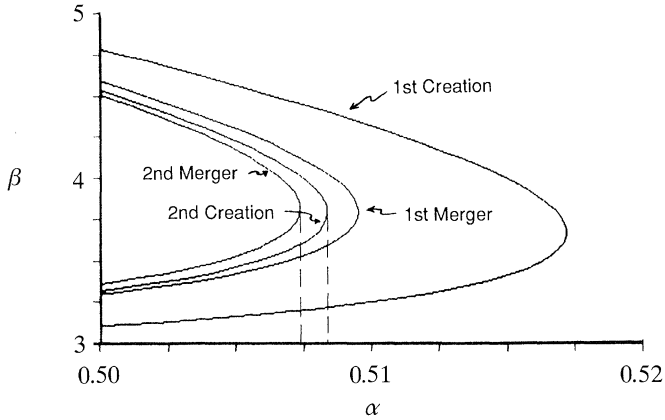

Figure 14. Saddle-node bifurcation sets for the first and second isolated periodic solution branches in the $\alpha\beta$ plane.

numerical simulations revealed period-doublings followed by undoublings, isolated oscillatory solution branches, Rössler type chaotic attractors and the formation of homoclinic/heteroclinic orbits. They termed these bifurcation structures (e.g. figure 8) as 'bubbles'. Not only did Funakoshi & Inoue (1988, 1990) find these bubbles in their numerical simulations of Miles's equations for surface waves in a cylindrical container, they also verified their existence in careful and well-controlled experiments. Knobloch & Weiss (1983) argued that this complex behaviour is naturally associated with the formation of homoclinic orbits when the eigenvalues of the saddle-point satisfy the approximate Sil'nikov inequality. The importance of homoclinic (or heteroclinic) orbits was established by Sil'nikov first for a third-order system of ordinary differential equations and was later generalized to higher dimensional systems. The hypotheses of the Sil'nikov (1970) theorem are: the system has a homoclinic orbit at a fixed point; the fixed point has one positive real eigenvalue σ_1, a complex conjugate pair of eigenvalues, $\lambda_2 = \sigma_2 + \mathrm{i}\omega_2 = \bar{\lambda}_3$, with negative real parts, and all the other eigenvalues $\lambda_4, \lambda_5, \ldots$, have negative real parts such that $\sigma_1 > 0 > \sigma_2 > \mathrm{Re}\,\lambda_4 \geqslant \ldots$. Sil'nikov then showed that whenever the eigenvalues satisfy the inequality

$$\delta \equiv |\sigma_2|/\sigma_1 < 1, \ \omega_2 \neq 0, \tag{21}$$

the Poincaré return map associated with the homoclinic orbit contains a countably infinite number of Smale's horseshoes. Each horseshoe contains an invariant Cantor set with an uncountable number of aperiodic orbits and a countably infinite number of periodic orbits of arbitrarily long periods. It also contains a dense orbit, i.e. an orbit that comes arbitrarily close to each point of the invariant set. The orbits created are all non-stable. These results are valid in an open interval of the parameter set containing the parameter value at homoclinicity.

The horseshoes themselves can generate different phenomena. They can generate very long transients, often referred to as 'transient' chaos. The existence of the horseshoes can also generate a 'strange attractor' (Guckenheimer & Holmes 1983), which itself is an invariant set, and the solution appears to be chaotic for all time.

In case $\delta > 1$, the system is predicted to have a stable periodic orbit on one side of the homoclinicity and no recurrent behaviour on the other. The period of the orbit tends to infinity as the homoclinicity condition is approached.

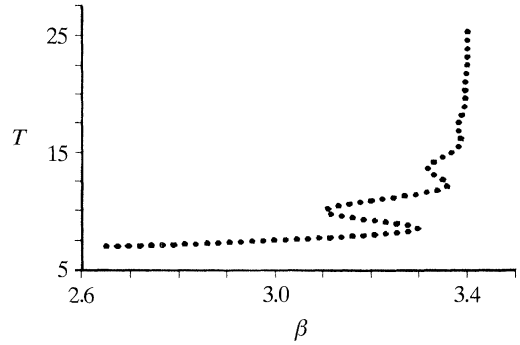

Figure 15. Period of the P_1 solution as a function of detuning; $\alpha = 0.5$.

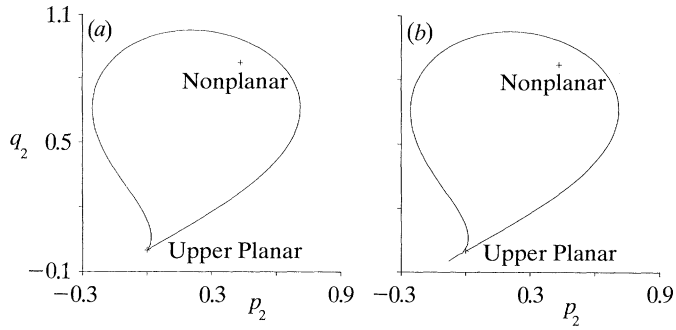

Figure 16. Unstable manifold of upper planar fixed point near the homoclinic orbit; $\alpha = 0.5$. (*a*) $\beta = 3.40$; (*b*) $\beta = 3.41$.

The results of Sil'nikov have to be appropriately modified if the system is invariant under some symmetry since the existence of a periodic orbit implies the existence of another orbit which is the image of the first under symmetry (Glendinning 1984). Furthermore, though the theorem predicts a drastic change in the behaviour of the system depending on whether $\delta < 1$ or $\delta > 1$, it has now been well established (Glendinning & Sparrow 1984; Mees & Sparrow 1987) that in a two-parameter family of system, no spectacular change in the behaviour is observed numerically as δ varies through one. This is because the neighbourhood in which the theorem is valid shrinks to zero as δ approaches one and this in turn suggests that a stable periodic orbit may be observed when $\delta < 1$ or that chaotic behaviour may be observed when $\delta > 1$.

For the string system, figure 15 has shown the possibility of the existence of a homoclinic orbit. Further numerical evidence is provided in figure 16 which shows one branch of the one-dimensional unstable manifold of the upper planar fixed point for $\alpha = 0.5$ and for frequencies, β, on either side of the critical value at which the homoclinic orbit exists. Notice that in both cases the manifold comes back very close to the fixed point itself but then heads toward opposite non-planar fixed points. The critical value of frequency β is found to be $\beta = 3.40266\ldots$, where the eigenvalues for the upper planar fixed point are $\sigma_1 = 0.4049$, $\lambda_{2,3} = -0.5 \pm 1.744\mathrm{i}$ and $\lambda_4 = -1.4049$. Clearly, $\delta = 0.5/0.4049 = 1.235 > 1$, and therefore, accounting for the reflection symmetry, Sil'nikov's theorem predicts the existence of periodic orbits on either side of the homoclinic orbit. Figure 17 shows one of the 'twin' limit cycles, at $\beta = 3.40$,

Figure 17

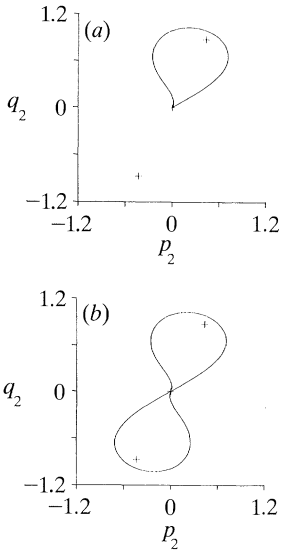

Figure 18

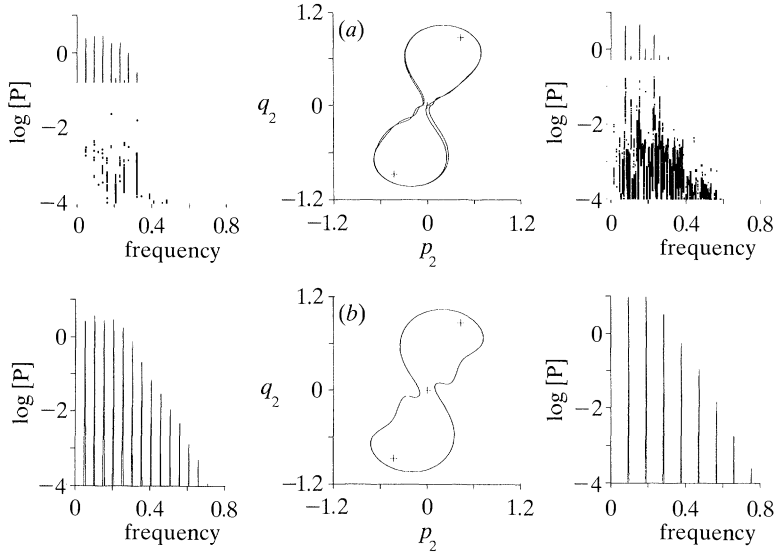

Figure 17. Limit cycles near the homoclinic orbit; $\alpha = 0.5$. (*a*) $\beta = 3.40$; (*b*) $\beta = 3.41$.

Figure 18. Multiple stable Lorenz type attractors; $\alpha = 0.5$, $\beta = 3.5$.

just before the formation of the homoclinic orbit as well as the single symmetric limit cycle, at $\beta = 3.41$, encompassing both non-planar fixed points along with the upper planar fixed point. Thus, the formation of the homoclinic orbit leads to a merger of the twin limit cycles into one large symmetric limit cycle. Also note (figure 15) that, for sufficiently large periods, the period T of the periodic solution approaches the vertical asymptote monotonically, as predicted by the theory.

It should be pointed out here that although $\delta > 1$ for the homoclinic orbit under consideration, the Sil'nikov theorem does not preclude much of the bifurcation structure except for arbitrarily close to the homoclinic bifurcations (Glendinning & Sparrow 1984). This is borne out by the results presented earlier and our numerical simulations, which show that the bifurcations sequence from the larger limit cycle beyond the homoclinicity point is also quite complex. Multiple branches of periodic solutions are found to exist on this side of the homoclinic orbit. Figure 18 shows two very different steady-state solutions existing at the same parameter values. The second branch of solutions undergoes a series of bifurcations that lead to the formation of a Lorenz type chaotic attractor. Figure 19 is a series of phase plots along with the spectra for $\alpha = 0.500$ for various detuning parameters and shows the formation of the Lorenz type chaotic attractor. The Lyapunov exponents for the Lorenz type attractor at $\alpha = 0.50$, $\beta = 3.80$ are found to be (0.048, 0.000, -0.967, -1.043) and the resulting Lyapunov dimension of the attractor is $D_{\mathrm{L}} = 2.050$.

(*f*) *Crisis: chaos quenching*

The non-constant steady-state solutions for the averaged equations of the truncated string system have been explained in sufficient detail for all values of damping $\alpha \geqslant 0.50$. For each value of damping, the solutions over the relevant frequency range have been discussed. As the damping is reduced further, it turns out that the Lorenz type attractors (periodic, chaotic, etc.) abruptly disappear over a

PHILOSOPHICAL TRANSACTIONS OF THE ROYAL SOCIETY A MATHEMATICAL, PHYSICAL & ENGINEERING SCIENCES

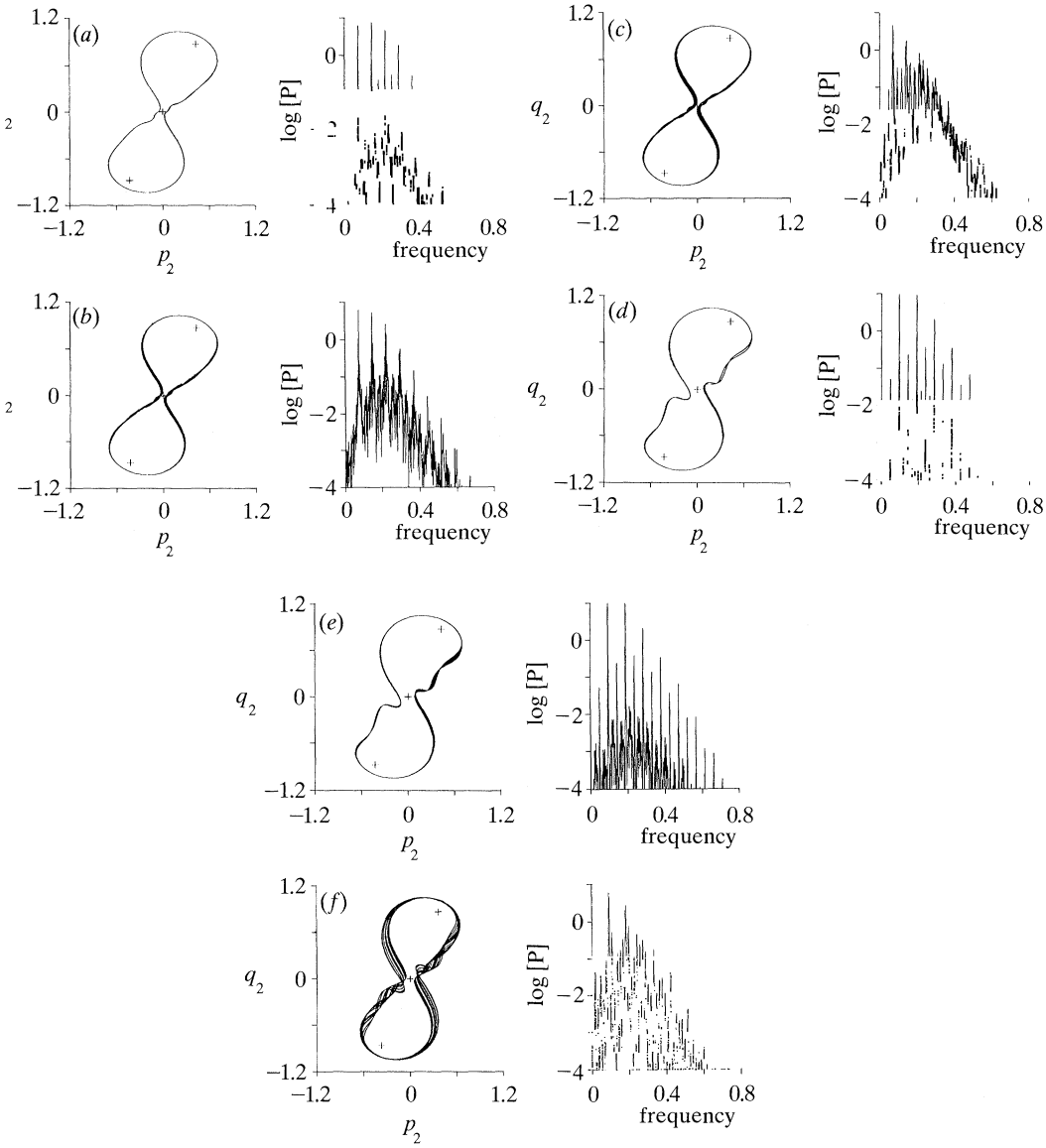

Figure 19. Phase plots and frequency spectra for Lorenz type attractors; $\alpha = 0.5$. (*a*) $\beta = 3.45$; (*b*) $\beta = 3.46$; (*c*) $\beta = 3.47$; (*d*) $\beta = 3.59$; (*e*) $\beta = 3.60$; (*f*) $\beta = 3.80$.

frequency interval. The only stable solution found in this interval is the lower planar constant solution. This phenomenon is first observed for $\alpha = 0.495$ and can only be explained through the introduction of the idea of a 'crisis' or a heteroclinic bifurcation.

Grebogi *et al.* (1983) have defined the concept of a boundary crisis. It involves a chaotic attractor coming into contact with its own basin boundary, resulting in the destruction of the attractor. Streit *et al.* (1988) found this chaos quenching in a parametrically excited two-degrees-of-freedom system, that is similar in many ways to the string system.

The importance of the stable manifold of the middle planar fixed point was

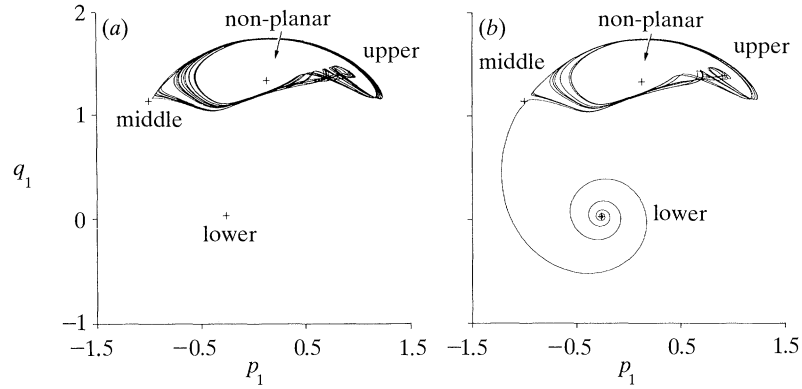

Figure 20. 'Crisis' in averaged equations for the string; $\alpha = 0.495$. (*a*) Lorenz type chaotic attractor, $\beta = 3.8$; (*b*) chaotic attractor destroyed by a crisis (transient chaos), $\beta = 3.89$.

stressed in §3*b*. It was argued there that this manifold separates the domains of attraction of the lower and upper planar fixed points. A more general statement can be made. The stable manifold of the middle planar solution forms the basin boundary between the attractors on opposite sides. On one side of the manifold almost every trajectory leads to the stable lower planar fixed point. On the other side almost every trajectory leads to the Lorenz type chaotic attractor that encircles both unstable non-planar fixed points as well as the unstable upper planar fixed point.

A crisis occurs when the chaotic attractor comes into contact with its basin boundary. In the present context, it means that the Lorenz type chaotic attractor comes into contact with the stable manifold of the middle planar fixed point. Because of the definition of the stable manifold, a trajectory that contacts the stable manifold must also contact the fixed point. Thus for dynamical systems, a boundary crisis can be thought of as an unstable saddle-type fixed point colliding with and destroying a chaotic attractor. After a crisis has occurred and the attractor destroyed, trajectories that used to lead to the attractor will remain, for a finite time, in the vicinity where the attractor existed (ghost of the chaotic attractor) but will eventually lead to the lower planar fixed point. Figure 20*a* shows the Lorenz type chaotic attractor and other relevant fixed points at a detuning value just before the boundary crisis. The attractor comes very close to the middle planar fixed point. At a slightly higher detuning, the attractor has grown sufficiently to collide with the saddle-type planar fixed point. Figure 20*b* clearly shows an attractor like object but it is only a transient. After staying around the ghost of the chaotic attractor the trajectory suddenly appears to collide with the fixed point and quickly converges to the lower planar stable fixed point. This is an example of the phenomenon termed 'transient chaos' (Parker & Chua 1987) in the literature.

As damping is reduced, the crisis points (i.e. the values of the detuning parameter β at which the crises occur) move steadily closer to the Hopf bifurcation points β_{1*} and β_{2*} (e.g. figure 4). Essentially the same sequence of events lead up to the crisis. The events are, however, compressed into a smaller detuning interval. Thus, as the damping is lowered, the frequency intervals over which the non-planar complex motions exist decrease, so much so that, for $\alpha = 0.25$ (the biggest damping value for which Miles (1984*a*) tried numerical integration), the critical frequencies at which crisis occurs essentially coincide with β_{1*} and β_{2*} and practically all initial conditions lead to the lower planar steady-state constant solution (figure 4).

Figure 21

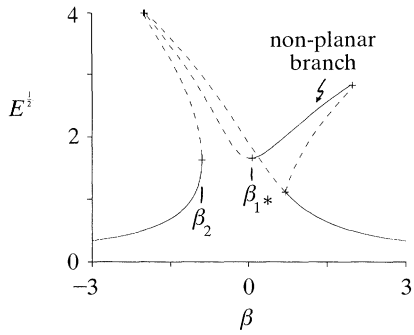

Figure 22

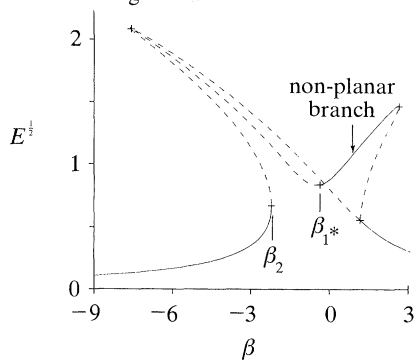

Figure 21. Constant amplitude response curve for the pendulum; $\alpha = 0.25$.

Figure 22. Constant amplitude response curve for the beam; $\alpha = 0.4797$.

(*g*) *Connections to similar systems*

As previously noted, the averaged equations for the string system differ only by a single nonlinear ratio from the averaged equations for a number of other physical systems including the spherical pendulum, and a beam. Many of the important features of the solutions for the string system are found for every member of the family. Works of Miles (1984*b*, *c*), Maewal (1986, 1987), and Funakoshi & Inoue (1988, 1990) have shown that both Rössler and Lorenz type chaotic attractors exist throughout the family.

Typical constant amplitude response curves for the spherical pendulum and the beam are shown in figures 21 and 22 respectively. The pendulum system is obtained from equations (14) by setting (A, B) to $(0.25, -0.75)$ while the beam system is obtained by setting (A, B) to $(3.491, -5.958)$. The values of damping, α, in figures 21 and 22 have been chosen to correspond with a damping value used in Miles (1984*b*) and Maewal (1986). The same damping will be used later in this section. There are several important differences between these response curves and the response curves for the string system. One clear difference is in the nature of nonlinear coefficients, A and B, such that for the pendulum and the beam system, the backbone curve for the planar branch and the backbone curve for the non-planar branch bend in different directions. As a result, when the non-planar solutions become unstable by Hopf bifurcation, there is an interval in frequency, $(\beta_2 - \beta_{1*})$, where there are no stable constant solutions. In this interval, the only attractors that exist are limit cycles and chaotic attractors. This makes finding interesting solutions using long time integration exceedingly easy when contrasted with the case of the string system. Almost every choice of initial conditions for frequencies in the interval $(\beta_2 - \beta_{1*})$ leads to periodic or chaotic solutions.

A more detailed investigation of Maewal's beam equations shows that multiple solution branches also exist for that system. Figure 23 shows a saddle-node bifurcation set in the $\alpha\beta$ plane corresponding to one of the creation and merger phenomena for an isolated periodic solution branch for the beam equations. It is important to note that while for every fixed α there are two saddle-node bifurcation frequencies at which the branch is created (annihilated) (compare with figure 12 for the string), only one (the larger of the two) is shown here. Similarly, only one of the saddle-node bifurcations where merger takes place is shown, though two exist for

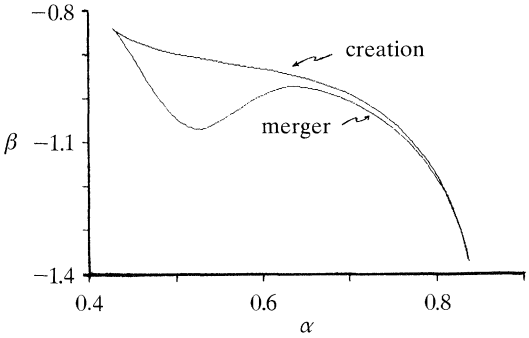

Figure 23. Saddle-node bifurcation set for isolated periodic solutions branch in the $\alpha\beta$ plane for the beam.

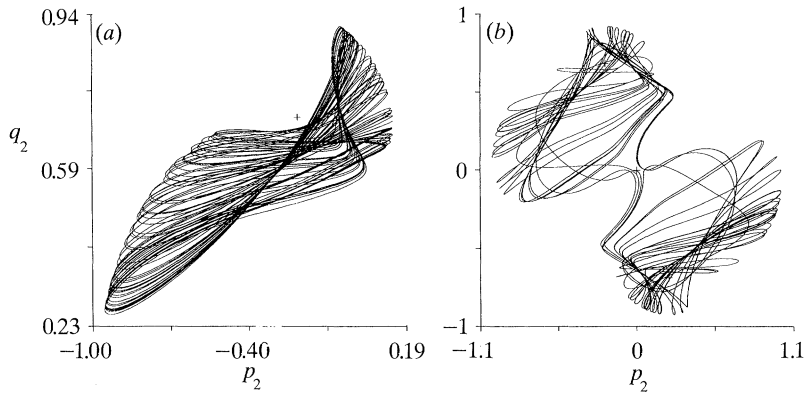

Figure 24. Merger of 'twin' Rössler type chaotic attractors resulting in a Lorenz type attractor for the beam; $\alpha = 0.4797$. (*a*) $\beta = -0.667$; (*b*) $\beta = -0.668$.

each α. This is essentially because the plot was generated using AUTO. Although AUTO is very powerful, it sometime has difficulty following branches when solution branches become very close. For the beam system, as α approaches 0.84, the creation and merger bifurcation branches come so close to each other that AUTO fails to be able to continue them effectively. If they were continued, both branches would have a turning point near $\alpha = 0.84$ where they would connect with the lower halves of the curves not shown. Thus, figure 23 shows that the beam system has an isolated branch just as the string system does. The fact that the creation and merger branches have turning points very close to each other indicates that the range of damping α for which the 'isolated' branch is truly isolated is very small.

The merger of the 'twin' non-planar attractors in the beam and the pendulum systems is a little different from that for the string system. For the two attractors to merge, unstable manifold of the upper planar fixed point must pass through the stable manifold. This implies that a homoclinic orbit is formed as the solutions merge. In the string system the Rössler type chaotic attractor reverse bifurcated back to a limit cycle solution before the merger. This scenario does not arise in either the beam or the pendulum problem. Figure 24 shows one of the 'twin' chaotic attractors in Maewal's beam equations just before merger, and the Lorenz type chaotic attractor created by the merger for a slightly different value of detuning. Figure 25 shows the corresponding attractors for Miles's pendulum equations. The

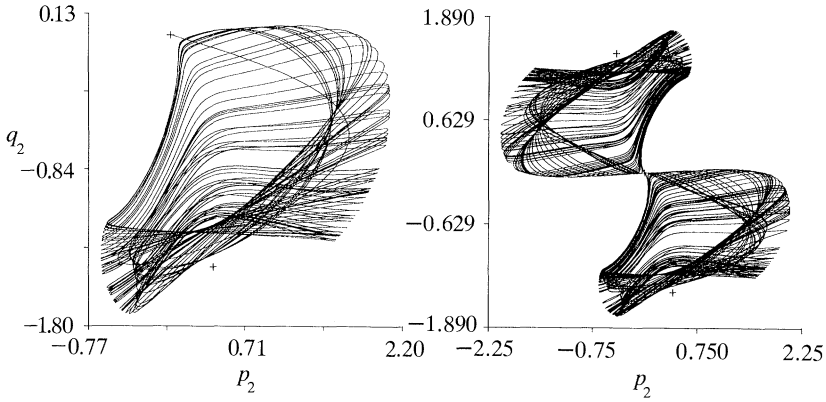

Figure 25. Merger of 'twin' Rössler type chaotic attractors resulting in a Lorenz type attractor for the pendulum; $\alpha = 0.25$; (*a*) $\beta = -0.1485$; (*b*) $\beta = -0.150$.

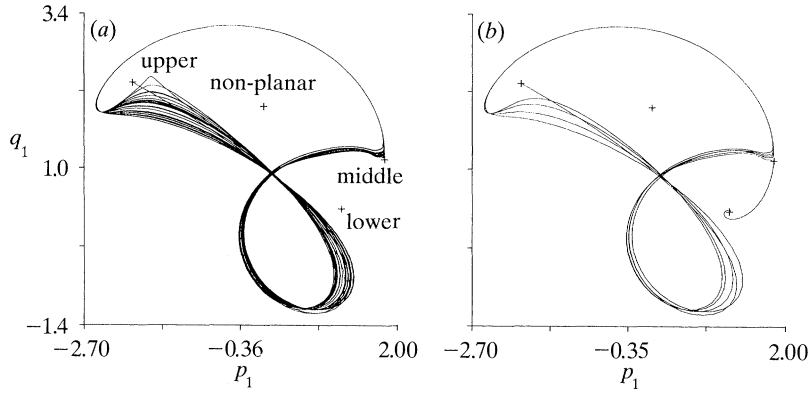

Figure 26. 'Crisis' for the pendulum; $\alpha = 0.25$. (*a*) Lorenz type chaotic attractor, $\beta = -0.967$; (*b*) transient chaos, $\beta = -0.969$.

crucial difference in behaviour can be explained in terms of the eigenvalue condition for the saddle-type fixed point, as specified by the Sil'nikov theorem. For the spherical pendulum with $A = 0.25, B = -0.75$ and damping $\alpha = 0.25$, the homoclinic orbit is formed at $\beta = -0.1495\ldots$. The upper planar fixed point is again a saddle-focus with eigenvalues $\sigma_1 = 0.8353$, $\lambda_{2,3} = -0.25 \pm 0.7815\mathrm{i}$ and $\lambda_4 = -1.3353$. Thus $\delta = 0.25/0.8353 = 0.299 < 1$, implying the existence of complex dynamics including homoclinic bifurcations, horseshoes, and transitions between Rössler and Lorenz type chaotic attractors.

Crisis in chaotic attractors also seems to be a phenomenon common to the entire family of equations. As mentioned earlier, the beam and pendulum equations have an interval in frequency β, (β_2, β_{1*}), where there are no stable constant solutions. For the values of α chosen, the solution branch emanating from the Hopf bifurcation at β_{1*} quickly gives rise to a chaotic attractor as β is reduced. This attractor grows rapidly as the turning point β_2 is approached (see figures 21 and 22). Reducing β past β_2, the lower and the middle planar fixed points are created. The crisis occurs very near the turning point in the constant amplitude response curves. Figure 26*a* shows the Lorenz type attractor and relevant fixed points for Miles's pendulum equations just prior to the boundary crisis. Figure 26*b* shows the transient behaviour immediately after the chaotic attractor is destroyed by a crisis. In the case of the

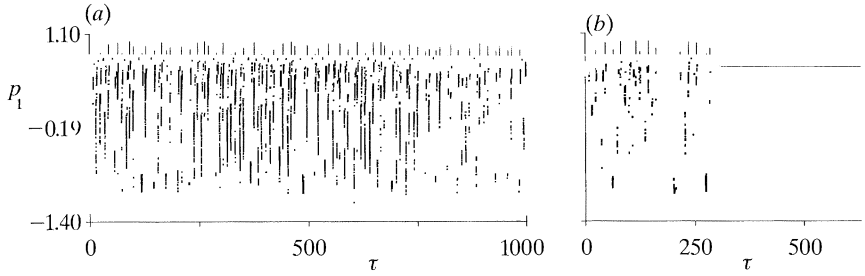

Figure 27. 'Crisis' for the beam; $\alpha = 0.4797$. (*a*) Sustained chaotic response, $\beta = -2.19$; (*b*) transient chaotic response, $\beta = -2.2$.

beam equations, the lower and the middle planar fixed points are created in the interior of the attractor making it difficult to demonstrate the crisis in the phase space. Thus, figure 27*a*, *b* display the crisis using the time response of the amplitude variable p_1.

Having studied the averaged system (14) for various solutions in the last two sections we now consider the non-autonomous equations governing the motion of the string. Solutions of the non-autonomous system are studied in light of what is known about the averaged system.

5. Dynamic response of strings

This section discusses the connection between solutions of the averaged equations and the corresponding solutions of the N-mode truncation of the string equations. An attempt is made to interpret the consequences of the various solutions of the averaged equations found in previous sections. For constant and periodic solutions, the infinite-time theorems in the method of averaging and the integral manifold theory allow some strong statements to be made concerning the connection between the two systems. However, at present there are no corresponding theorems that apply to chaotic solutions of the averaged system. Furthermore, even in the case of constant and periodic solutions of the averaged equations, the available theorems make predictions that are valid only for 'small enough' $\hat{\epsilon}$. Because the parameter value that is small enough is unknown, the averaging results may not be valid for problems of physical interest. Many of these issues are addressed when discussing the results of numerical investigations of the truncated string equations.

Direct study of the non-autonomous system confirms the existence of many of the phenomena observed in the averaged system. The non-autonomous system is found to exhibit almost periodic motions (i.e. motion on a 2-torus), torus-doubling bifurcations, multiple solution branches, merger of symmetric tori, chaotic attractors, and chaos quenching or crisis.

(*a*) *Review of theorems in averaging*

In the interest of completeness and for ease in subsequent discussions, the essential steps in the development of the averaged equations for the N-mode system given in §2 are, again, spelled out below.

An N-mode truncation of the string system is given in equations (6). These equations are transformed into the 'standard form', suitable for the application of

the method of averaging, by the van der Pol transformations (7), resulting in the equations (8). The averaged equations (9) are obtained from equations (8) by using a near-identity transformation, and then neglecting or dropping terms of $O(\hat{\epsilon}^2)$ and higher.

In the following, the basic results relating solutions of the averaged system (9) to those of the system (8) are discussed after presenting the essential theorems (Hale 1963, 1969).

(i) *Infinite-time averaging theorem*

Suppose that the averaged system (9) has a hyperbolic constant solution (i.e. a solution with eigenvalues away from the imaginary axis), $(\boldsymbol{A}_n^0, \boldsymbol{B}_n^0)$, $n = 1, 2, \ldots, N$. Then, for each $\hat{\epsilon}$, $0 < \hat{\epsilon} < \epsilon_1^*$ and some $\epsilon_1^* \ll 1$, there is a 2π-periodic solution, $(\hat{\boldsymbol{A}}_n(\tau_1, \hat{\epsilon}), \hat{\boldsymbol{B}}_n(\tau_1, \hat{\epsilon}))$, $n = 1, 2, \ldots, N$, of equations (8) which lies near $(\boldsymbol{A}_n^0, \boldsymbol{B}_n^0)$, $n = 1, 2, \ldots, N$ and $\|\hat{\boldsymbol{A}}_n(\tau_1, \hat{\epsilon}) - \boldsymbol{A}_n^0\| + \|\hat{\boldsymbol{B}}_n(\tau_1, \hat{\epsilon}) - \boldsymbol{B}_n^0\| \to 0$ is $\hat{\epsilon} \to 0$. The stability of the solution $(\hat{\boldsymbol{A}}_n(\tau_1, \hat{\epsilon}), \hat{\boldsymbol{B}}_n(\tau_1, \hat{\epsilon}))$, $n = 1, 2, \ldots, N$, is the same as that of the constant solution $(\boldsymbol{A}_n^0, \boldsymbol{B}_n^0)$, $n = 1, 2, \ldots, N$ with respect to the averaged system.

The original oscillators (6) then clearly have a 2π-periodic solution $z_n(\tau_1)$ which is approximated by

$$z_n(\tau_1) = \boldsymbol{A}_n^0 \cos n\tau_1 + \boldsymbol{B}_n^0 \sin n\tau_1 + O(\hat{\epsilon}), \quad n = 1, 2, \ldots, N. \tag{22}$$

(ii) *Integral manifold theorem*

Suppose that the averaged system (9) has a hyperbolic limit cycle or steady-state periodic solution (i.e. a solution with $(4N-1)$ Floquet multipliers away from the unit circle),

$$\hat{\boldsymbol{A}}_n = \hat{\boldsymbol{A}}_n^*(\theta), \quad \hat{\boldsymbol{B}}_n = \hat{\boldsymbol{B}}_n^*(\theta), \quad n = 1, 2, \ldots, N, \tag{23}$$

where $\hat{\boldsymbol{A}}_n^*$ and $\hat{\boldsymbol{B}}_n^*$ are 2π-periodic in θ and $\theta \equiv \hat{\epsilon}\Omega\tau_1$ for some $\Omega > 0$. Then, for each $\hat{\epsilon}$, $0 < \hat{\epsilon} < \epsilon_2^*$ and some $\epsilon_2^* \ll 1$, the solution of equations (8) is of the form

$$\hat{\boldsymbol{A}}_n = \hat{\boldsymbol{A}}_n(\theta, \tau_1, \hat{\epsilon}), \quad \hat{\boldsymbol{B}}_n = \hat{\boldsymbol{B}}_n(\theta, \tau_1, \hat{\epsilon}), \quad n = 1, 2, \ldots, N. \tag{24}$$

The solution (24) lies on an integral manifold S which is a surface 2π-periodic in θ and 2π-periodic in τ_1. The manifold S lies close to the cylinder $\{(\hat{\boldsymbol{A}}_n^*(\theta), \hat{\boldsymbol{B}}_n^*(\theta)), n = 1, 2, \ldots, N\} \times \tau_1$ and coincides with it as $\hat{\epsilon} \to 0$. The stability of the integral manifold S is the same as that of the limit cycle of the averaged system.

The motion of the coupled oscillators (6), for a parameter set at which the averaged equations have a limit cycle, is then

$$z_n(\theta, \tau_1, \hat{\epsilon}) \equiv \hat{\boldsymbol{A}}_n(\theta, \tau_1, \hat{\epsilon}) \cos n\tau_1 + \hat{\boldsymbol{B}}_n(\theta, \tau_1, \hat{\epsilon}) \sin n\tau_1, \quad n = 1, 2, \ldots, N. \tag{25}$$

The motion is amplitude modulated with basic period 2π. The period of modulations is determined by the slow timescale and, for small $\hat{\epsilon}$, is very large, compared with 2π. The modulations are, therefore, very slow in the natural time τ_1.

Thus, the constant and periodic solutions of the averaged equations (9) provide a first-order approximation to 2π-periodic and almost periodic solutions of the oscillators (6). These approximations are valid for small enough $\hat{\epsilon}$.

In addition to results relating the constant and periodic steady-state motions of the averaged equations, some other results relate transient solutions of the averaged equations lying on the stable and unstable manifolds of the steady-state solutions to the corresponding solutions for the original equations. We do not state them here and the interested reader can consult Guckenheimer & Holmes (1983).

PHILOSOPHICAL TRANSACTIONS OF THE ROYAL SOCIETY A MATHEMATICAL, PHYSICAL & ENGINEERING SCIENCES

(iii) *Interpretation of averaging results for the string*

The averaged equations for the N-mode truncation of the string equations were given explicitly in §2. There it was shown that only the modal amplitudes $(\boldsymbol{A}_r, \boldsymbol{B}_r)$ corresponding to the mode in resonance may have nonzero solutions. All the other modal amplitudes $(\boldsymbol{A}_n, \boldsymbol{B}_n)$, $n = 1, 2, \ldots, r-1, r+1, \ldots, N$ decay exponentially and their only steady-state solution is the zero solution. Sections 3 and 4 were devoted to a detailed investigation of steady-state constant, periodic as well as aperiodic solutions of the averaged equations for the modal amplitudes $\boldsymbol{A}_r$ and $\boldsymbol{B}_r$ as a function of the frequency of excitation β and the damping α.

The averaged equations for the resonant mode have been found to possess 'planar' as well as 'non-planar' constant solutions. The N-mode truncation of the string then has a corresponding periodic solution

$$\left.\begin{aligned} z_r &= \boldsymbol{A}_r^0 \cos r\tau_1 + \boldsymbol{B}_r^0 \sin r\tau_1 + O(\hat{\epsilon}), \\ z_n &= O(\hat{\epsilon}), \quad n = 1, 2, \ldots, r-1, r+1, \ldots, N. \end{aligned}\right\} \tag{26}$$

Thus the primary motion of the string is in the resonantly excited mode, is periodic with period 2π, and is, essentially, planar (i.e. in the plane of forcing) or non-planar, as predicted by the averaging analysis.

Similar statements can be made when the averaged equations exhibit limit cycle solutions. The truncated string equations then have an amplitude modulated motion which is essentially in the mode directly excited. The motion is given by

$$\left.\begin{aligned} z_r &= \hat{\boldsymbol{A}}_r^*(\theta) \cos r\tau_1 + \hat{\boldsymbol{B}}_r^*(\theta) \sin r\tau_1 + O(\hat{\epsilon}), \\ z_n &= O(\hat{\epsilon}), \quad n = 1, 2, \ldots, r-1, r+1, \ldots, N. \end{aligned}\right\} \tag{27}$$

In fact, due to the nature of equations (6), it is easy to see that $z_r \equiv 0$, $n = 1, 2, \ldots, r-1, r+1, \ldots, N$, is always a solution. Thus, the non-resonantly excited modes remain identically zero if started with zero initial conditions and the motion is completely restricted to the rth mode. This observation will be used in the subsequent investigations of the non-autonomous string system.

(iv) *Unresolved aspects*

Averaging theory and the theory of integral manifolds only partly answer the questions concerning the connection between the solutions of the averaged system and those of the non-autonomous system. One unresolved aspect involves chaotic attractors in the averaged system. At present, there are no infinite-time results relating aperiodic, asymptotic (in time) behaviour in the averaged equations to the dynamics of the non-autonomous system. Even though there is no mathematical justification for assuming that a chaotic attractor in the averaged system has a chaotic counterpart for the non-autonomous system, one has the mystical hope that there is such a connection. Heuristically, one could argue that if the chaotic attractor of the averaged system is sufficiently hyperbolic (perhaps defined though the use of Lyapunov exponents) a corresponding chaotic attractor should exist in the non-autonomous system for small enough $\hat{\epsilon}$.

Another question left unanswered in the averaging theory is its range of applicability. The relevant theorems predict the existence of some $\hat{\epsilon}^*$ such that the results are valid for all $\hat{\epsilon}$, $\hat{\epsilon} < \hat{\epsilon}^*$. Very few analytical investigations (Schapiro &

PHILOSOPHICAL TRANSACTIONS OF THE ROYAL SOCIETY A MATHEMATICAL, PHYSICAL & ENGINEERING SCIENCES

Sethna 1977) exist on the estimates of small parameter $\hat{\epsilon}^*$ for which the solutions of the averaged equations (9) have quantitative as well as qualitative correspondence with the solutions of the original system.

To at least partly address the aforementioned questions, the $O(\hat{\epsilon}^2)$ terms, which were neglected to obtain the averaged equations, can be viewed as small 2π-periodic perturbations to the averaged system. The size of $\hat{\epsilon}$ determines the strength of these perturbations. The persistence of a solution of the averaged equations in the presence of periodic perturbations depends on the strength of the perturbations as well as on the stability (or, more generally, the hyperbolicity) of the solution. This viewpoint is followed through in the discussions in the next section (also see Bajaj & Johnson 1990; Bajaj & Tousi 1990).

(*b*) *Averaging revisited*

The averaged equations can be interpreted in a slightly different manner. The non-autonomous system in standard form (8) can also be written as an extended autonomous system

$$\begin{aligned} \boldsymbol{A}'_n &= \hat{\epsilon}\boldsymbol{f}_{10}(\boldsymbol{A},\boldsymbol{B}) + \hat{\epsilon}^2\boldsymbol{f}_{11}(\boldsymbol{A},\boldsymbol{B},\Omega,\hat{\epsilon}),\\ \boldsymbol{B}'_n &= \hat{\epsilon}\boldsymbol{f}_{20}(\boldsymbol{A},\boldsymbol{B}) + \hat{\epsilon}^2\boldsymbol{f}_{21}(\boldsymbol{A},\boldsymbol{B},\Omega,\hat{\epsilon}), \quad n = 1,2,\ldots,N, \quad \Omega' = 1, \end{aligned} \tag{28}$$

where $\boldsymbol{f}_{i1}, i = 1,2$ are 2π-periodic in Ω. The averaged system is then the uncoupled set of equations

$$\boldsymbol{A}'_n = \hat{\epsilon}\boldsymbol{f}_{10}(\boldsymbol{A},\boldsymbol{B}), \quad \boldsymbol{B}'_n = \hat{\epsilon}\boldsymbol{f}_{20}(\boldsymbol{A},\boldsymbol{B}), \quad n = 1,2,\ldots,N, \quad \Omega' = 1. \tag{29}$$

Clearly, limit cycle solutions of the first two sets of equations in (29) imply a 2-torus for the system (29) and the integral manifold theorem states that the system (28) also has a 2-torus (the integral manifold S) at least for small enough $\hat{\epsilon}$. The actual nature of motion on the torus is not specified. The invariant torus of system (28) exists if the torus of system (29) is sufficiently hyperbolic. The occurrence of small denominators requires the imposition of some strong conditions of irrationality between the frequencies involved in the torus to ensure the existence of quasi-periodic behaviour on the torus (Iooss 1979). As a suitable parameter in the system is varied, these conditions may be violated resulting in frequency locking, that is, periodic orbits on the torus. The parameter variation may also produce conditions which lead to the destruction of the torus and to chaotic behaviour, as discussed by Aronson *et al.* (1982) as well as Kaneko (1984).

In recent years many investigators, including Miles (1984*a*, *b*, *c*), Maewal (1986, 1987), Johnson & Bajaj (1989) and Tousi & Bajaj (1985), have found cascades of period-doubling bifurcations (or torus-doubling bifurcations, if the averaged equations are cast in the form of equations (29)) leading to chaos in the averaged system. This implies a series of torus-doubling bifurcations in the corresponding non-autonomous systems. However, at the bifurcation point, the torus for system (29) is non-hyperbolic and therefore the integral manifold theory does not apply. In fact, the small parameter ϵ_2^*, for which the theorem is valid, quickly decreases as the parameter of interest moves closer to its critical value. Various numerical experiments on systems of this type show (Kaneko 1984; Arneodo *et al.* 1983) that there is an interruption of the cascade of torus-doubling before the chaotic behaviour arises. Coullet has related this to the 'instability of the scenario of torus-doubling'. He points out that a bifurcation of a torus is by itself unstable. The existence of a clean transition requires rather restrictive conditions (Chenciner & Iooss 1979) and

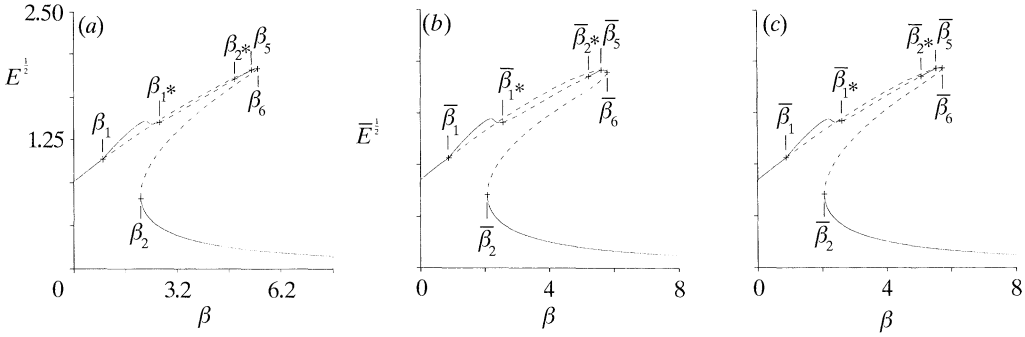

Figure 28. Response curve for 2π-periodic solutions of the string; $\alpha = 0.513$. (*a*) Prediction by averaging; (*b*) direct solutions, $\epsilon = 0.1$; (*c*) direct solutions, $\epsilon = 0.01$.

when these are not satisfied a 'fuzzy bifurcation' occurs. The parameter domain of fuzziness extends on both sides of the 'clean' transition point when the invariant tori are not sufficiently hyperbolic. As a consequence, the last steps in the torus-doubling cascade to chaos disappear in this fuzziness. As the small parameter $\hat{\epsilon}$ is decreased, the number of steps in the cascade, before it is interrupted, increase and Kaneko (1984) has investigated the scaling behaviour numerically for some coupled maps. He has also studied the mechanisms of this interruption from the viewpoints of the renormalization group approach, the fractalization of torus and the intermittent-like transition.

From the above discussion it is clear that, at least for small enough $\hat{\epsilon}$, the period-doubling bifurcation in the averaged equations (29) persists for the original system (28). The cascade of torus-doublings for the original equations is, however, interrupted before the chaotic behaviour arises. Furthermore, because of the fuzzy nature of the transition points, the parameter range for the existence of a certain kind of steady-state behaviour is expected to be different in the two cases. These various observations are completely borne out by the results for the truncated string system.

(*c*) *Constant amplitude or periodic solutions of the string*

Rather than appealing to the method of averaging to find approximations to periodic solutions of the N-mode truncation (equations (6)), and also in order to evaluate some of the issues discussed above, solutions to equations (6) are now directly investigated. A single-mode approximation ($N = 1$) is used in these studies for the case when the forcing frequency is near the lowest linear natural frequency ($r = 1$). Later some comments about the one-mode truncation will be made.

A branch continuation algorithm (Keller 1977) was used to find 2π-periodic solution branches of the system (6) as a function of β for fixed α, ϵ, and s. The emphasis was on the values of damping α for which the averaged equations possess limit cycle solutions. Figure 28*a–c* shows the constant amplitude response curves for parameters $\alpha = 0.513$, and $s = 0.1$. Here $\bar{E}$ represents the norm of the 2π-periodic solution defined by

$$\bar{E} = \frac{1}{2\pi}\int_0^{2\pi} (\boldsymbol{z}_r \cdot \boldsymbol{z}_r + \dot{\boldsymbol{z}}_r \cdot \dot{\boldsymbol{z}}_r)\, \mathrm{d}\tau_1.$$

Both the planar and the non-planar periodic solution branches are identified. The response curves of the non-autonomous system are sufficiently similar to those of the averaged equations that the same notation is used to describe the bifurcation points

PHILOSOPHICAL TRANSACTIONS OF THE ROYAL SOCIETY A MATHEMATICAL, PHYSICAL & ENGINEERING SCIENCES

of the two systems. The bifurcation points for the non-autonomous system are distinguished from those for the averaged system by an overbar. The stability of the periodic solutions is determined by the eigenvalues (Floquet multipliers) of the associated monodromy matrix. The unstable planar solution branch between the turning points arises due to one Floquet multiplier leaving the unit circle through $+1$. The same is true for the bifurcation points where the planar branch becomes unstable and gives rise to 2π-periodic non-planar solutions. The instability in the non-planar solution branch arises at $\bar{\beta}_{1*}$ and $\bar{\beta}_{2*}$ due to a complex-conjugate pair of Floquet multipliers leaving the unit circle.

The first curve (figure 28*a*) is the one predicted by the averaged equations. The second (figure 28*b*) and the third (figure 28*c*) response curves were obtained directly from the non-autonomous system (6) with $\epsilon = 0.1$, and $\epsilon = 0.01$ respectively. The correspondence between the solutions obtained from the non-autonomous system and those from the averaged system is quite good. As is expected, the correspondence improves as ϵ is reduced.

Although the response curves shown in figure 28 agree qualitatively, there are some quantitative differences. In particular, the bifurcation points for the non-autonomous system are somewhat shifted from the bifurcation points obtained using the averaged equations. This means that even though, at a particular value of ϵ, the averaged equations (13) may predict a stable 2π-periodic solution of the truncated string equations (6), the truncated string equations may in fact exhibit a stable almost periodic solution (i.e. a stable torus solution). It is important to recognize that the asymptotic method of averaging makes predictions that are valid provided that $\hat{\epsilon}$ is sufficiently small. The range of validity in $\hat{\epsilon}$ shrinks rapidly as bifurcation points are approached because solutions become non-hyperbolic at bifurcation points. Numerical evidence seems to suggest (Bajaj & Johnson 1990) that the difference between the bifurcation points behaves like $O(\hat{\epsilon}^{\frac{1}{2}})$ as $\hat{\epsilon} \to 0$. In fact for sufficiently small $\hat{\epsilon}$, it is found that, qualitatively, the response curves and the bifurcation set for a $(\alpha, \hat{\epsilon})$ pair are similar to another $(\alpha, \hat{\epsilon})$ pair with lower damping and higher $\hat{\epsilon}$. Thus, lowering damping α very much acts like increasing the forcing amplitude $\hat{\epsilon}$.

(*d*) *Almost periodic and aperiodic solutions:* $\epsilon = 0.1$, *investigation*

In parameter regions where the averaged equations have limit cycle solutions, the truncated string equations are expected to exhibit amplitude modulated motions. These equations (6) were integrated for $\epsilon = 0.1$, and various values of damping α and detuning β until a steady-state was reached. A particular value of ϵ was chosen to facilitate the comparison between the actual solutions and those predicted by the averaging analysis.

At $\epsilon = 0.1$, there are many similarities between the various steady-state solutions of the averaged system and those for the truncated string system. Major differences, however, also exist. A previous section demonstrated that as far as the constant amplitude solutions are concerned, the differences seem to be quantitative rather than qualitative except close to bifurcation points. For more complex solutions, however, there are differences that result in qualitative changes in the bifurcation sequence.

For $\alpha = 0.55$, the averaged equations only have a stable limit cycle branch joining the Hopf bifurcation points $(\beta_{1*}, \beta_{2*}) \equiv (2.8675, 3.8059)$. The truncated string equations are found to possess a stable 2-torus (or almost periodic motion) except that it exists over the frequency interval $(\bar{\beta}_{1*}, \bar{\beta}_{2*}) \equiv (2.6287, 4.1809)$. Clearly, over

PHILOSOPHICAL TRANSACTIONS OF THE ROYAL SOCIETY A MATHEMATICAL, PHYSICAL & ENGINEERING SCIENCES

the frequency intervals $(\bar{\beta}_{1*}, \beta_{1*})$ and $(\beta_{2*}, \bar{\beta}_{2*})$ the predictions of averaging are qualitatively different from the actual response of the system. This is consistent with the observations previously made for solutions near transition points. In the present case, the $O(\hat{\epsilon}^2)$ terms dropped in the averaging analysis have destabilized the 2π-periodic solution into a 2-torus.

As the damping is lowered, many more types of solutions and bifurcations such as torus-doublings, homoclinicity, chaotic attractors, etc., arise. Rather than creating a catalogue of differences, we here concentrate on some general features of the response. These are essentially dictated by the bifurcation sequences as a function of the system parameters.

One qualitative difference in the bifurcation sequence is a consequence of the movement of bifurcation points. As previously shown, the extent to which bifurcation points are shifted increases as $\hat{\epsilon}$ is increased. It is reasonable to expect that different types of bifurcations are affected to different extents by the inclusion of the perturbation terms. One type of bifurcation may be favoured while another may be less favoured, that is, the $O(\hat{\epsilon}^2)$ perturbations may stabilize some solutions and destabilize others. Thus, it is conceivable that this unequal shifting or sensitivity to perturbations may even alter the bifurcation sequence.

Evidence of this kind of behaviour can be found in the truncated string example. Recall that in the averaged system, periodic solutions in the isolated branch period-doubled *ad infinitum* to form a Rössler type chaotic attractor. Then, as α was reduced, a homoclinic orbit was formed. For $\epsilon = 0.1$, however, the truncated string equations have a different sequence of bifurcations. No Rössler type chaotic attractor is observed, rather the isolated branch has only one torus-doubling before the formation of a homoclinic orbit (of the Poincaré map). A homoclinic orbit of the Poincaré map implies a torus with an infinite winding number. The homoclinic orbit gives rise to a symmetric stable torus which, after several bifurcations, results in the formation of a Lorenz type chaotic attractor.

(i) *$\alpha = 0.513$ comparison*

To study the connection between the solutions of the averaged system and those for the non-autonomous system further, the truncated string system is investigated as a function of β for a value of damping at which the averaged system possesses a chaotic attractor, namely, $\alpha = 0.513$. As discussed earlier, bifurcation points for the truncated string equations are shifted when compared with those for the averaged system. This shifting is not only in β but in α as well, as is clearly demonstrated by the fact that this value of damping ($\alpha = 0.513$) yields a bifurcation sequence in the truncated string equations similar to the bifurcation sequence in the average system with a lower damping value (perhaps $\alpha \approx 0.5$, see figure 11).

The Hopf bifurcation from the non-planar 2π-periodic solution at $\bar{\beta}_{1*}$ gives rise to an almost periodic or 2-torus solution. Figure 29 shows for $\beta = 2.8$ the time history of the non-planar component as well as the Poincaré section of the solution. The Poincaré section also shows the relevant fixed point of the Poincaré map identifying the unstable 2π-periodic solution. This torus becomes unstable and torus-doubles as shown in figure 30 ($\beta = 2.9$). Just as the Hopf branch for the averaged equations undergoes a saddle-node bifurcation and merges with an isolated branch, the 2-torus solution branch arising in the truncated string equations due to Hopf bifurcation from the non-planar 2π-periodic solution appears to undergo a similar saddle-node bifurcation. This is evident from the fact that there is an interval in β where the Hopf

PHILOSOPHICAL TRANSACTIONS OF THE ROYAL SOCIETY A MATHEMATICAL, PHYSICAL & ENGINEERING SCIENCES

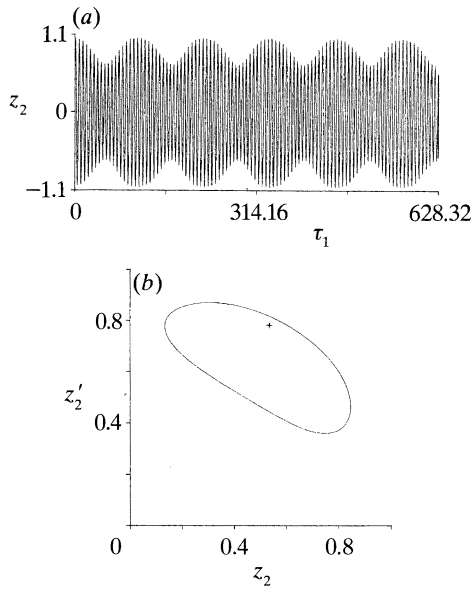

Figure 29. Almost periodic response (2-torus) for the string; $\alpha = 0.513$, $\beta = 2.8$, $\epsilon = 0.1$. (*a*) Time response, (*b*) Poincaré section.

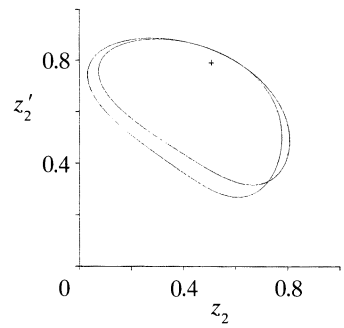

Figure 30. Almost periodic response (torus-doubled) for the string; $\alpha = 0.513$, $\beta = 2.9$, $\epsilon = 0.1$.

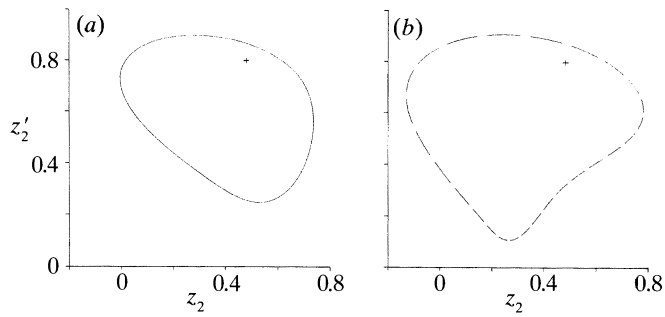

Figure 31. Multiple tori; $\alpha = 0.513$, $\beta = 3.0$, $\epsilon = 0.1$. (*a*) Hopf branch, (*b*) isolated branch.

branch ceases to exist. Also, there is an interval where multiple tori exist. Figure 31 shows Poincaré sections of two different tori at the same frequency ($\beta = 3.0$). The resemblance of the Poincaré sections of the solutions in the two branches to those of

PHILOSOPHICAL TRANSACTIONS OF THE ROYAL SOCIETY A MATHEMATICAL, PHYSICAL & ENGINEERING SCIENCES

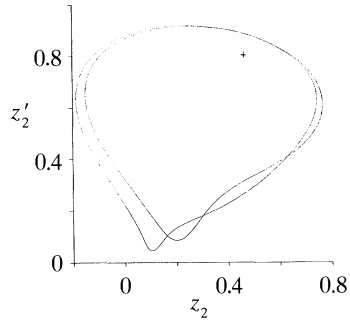

Figure 32. Torus-doubled solution in the isolated branch; $\alpha = 0.513$, $\beta = 3.08$, $\epsilon = 0.1$.

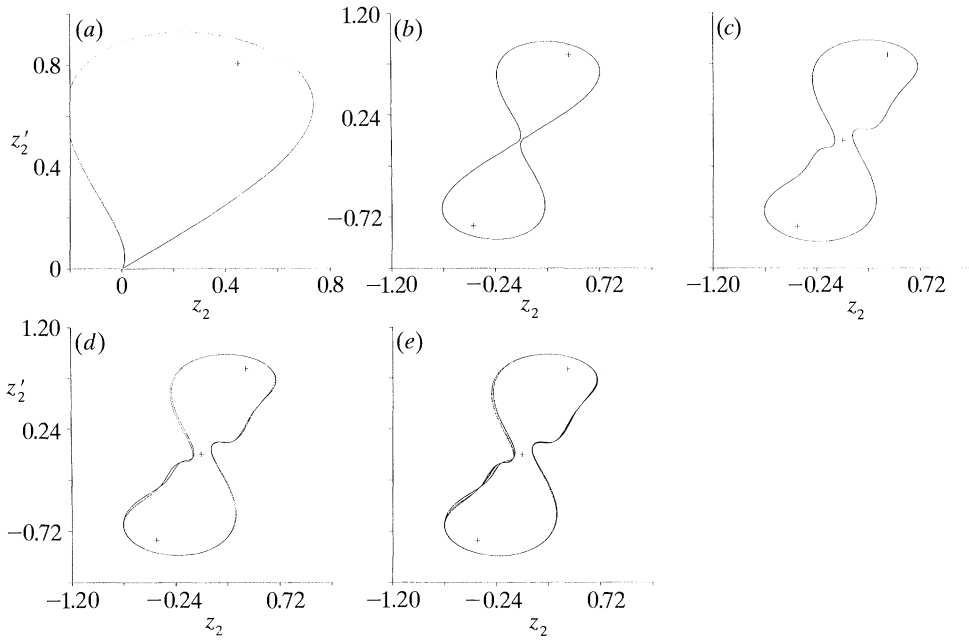

Figure 33. Poincaré sections of attractors leading to the Lorenz type attractor via homoclinic orbit; $\alpha = 0.513$, $\epsilon = 0.1$. (*a*) $\beta = 3.16$, (*b*) $\beta = 3.17$, (*c*) $\beta = 3.3$, (*d*) $\beta = 3.31$, (*e*) $\beta = 3.315$.

the solutions of the averaged system on the Hopf (fig. 4 in Johnson & Bajaj 1989) and isolated branches (figure 9*a*) is quite remarkable. It may be important to point out that for $\alpha = 0.513$, the two solution branches in the averaged system were isolated, whereas the branches for the truncated string system are already merged.

Recall that the isolated branch of the averaged system undergoes a cascade of period-doubling bifurcations as the frequency β is varied, resulting in the creation of a Rössler type chaotic attractor. The twin chaotic attractors then reverse bifurcate back to limit cycles which merge to form a homoclinic orbit. The homoclinic orbit finally gives rise to a single symmetric limit cycle that after a series of bifurcations results in the formation of a Lorenz type chaotic attractor. At this value of ϵ and s, the non-autonomous system does not possess a Rössler type chaotic attractor. Instead, the 2-torus in the isolated branch only torus-doubles once before the formation of a homoclinic orbit (of the Poincaré map). Figure 32 shows the Poincaré section of the T_2 (i.e. torus-doubled) solution for $\beta = 3.08$. As is the case in the

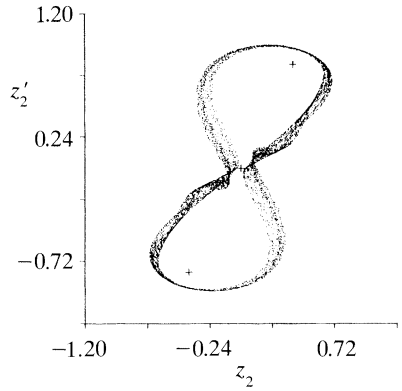

Figure 34. Section of Lorenz type chaotic attractor; $\alpha = 0.513$, $\beta = 3.4$, $\epsilon = 0.1$.

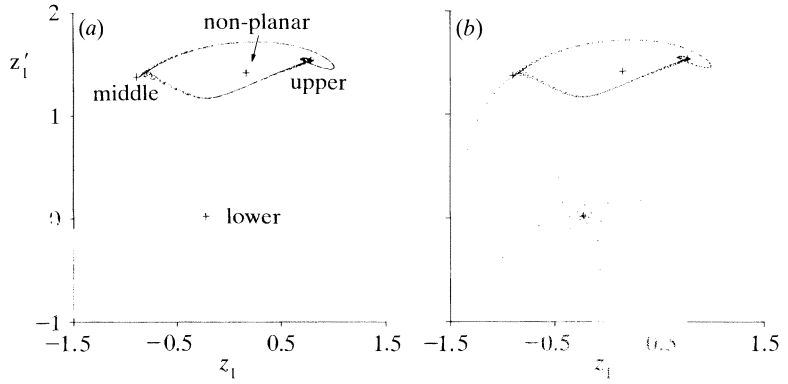

Figure 35. 'Crisis' in truncated string equations; $\alpha = 0.5$, $\epsilon = 0.1$. (*a*) Poincaré section of the chaotic attractor, $\beta = 4.5$; (*b*) Poincaré section displaying transient chaos, $\beta = 4.49$.

averaged system, the homoclinic orbit results from the merger of its symmetric twins and gives rise to a larger 2-torus solution encompassing both non-planar fixed points. Figure 33 shows a sequence of Poincaré sections leading to the merger of the twin tori. This larger solution, after a few torus-doubling bifurcations, leads to the formation of a Lorenz type chaotic attractor. Figure 34 shows, at $\beta = 3.4$, the chaotic attractor that is formed after the torus is destroyed. The Lyapunov exponents for this chaotic attractor also can be computed and are $(0.003, 0, 0, -0.066, -0.069)$, which corresponds to $D_L = 3.045$. Thus, there is chaotic dynamics present in the one-mode truncation of the string and, at least for $\epsilon = 0.1$, the chaotic attractor arises due to torus breakdown via the process of torus-doubling bifurcations.

(ii) *Crisis*

The chaotic attractor in the averaged equations was shown to undergo a boundary 'crisis', in which the attractor touches its basin boundary and is destroyed. For $\epsilon = 0.1$, $s = 0.1$, the non-autonomous system also exhibits a crisis. Figure 35*a* shows for $\beta = 4.5$ the Poincaré section of a Lorenz type chaotic attractor along with the relevant fixed points (i.e. the 2π-periodic solutions) of the Poincaré map just before the crisis. Figure 35*b* shows for only slightly different β, $\beta = 4.49$, the Poincaré section of the transient chaos once the chaotic attractor has been destroyed. In this figure, the dot size has been enlarged to highlight the points that spiral down toward

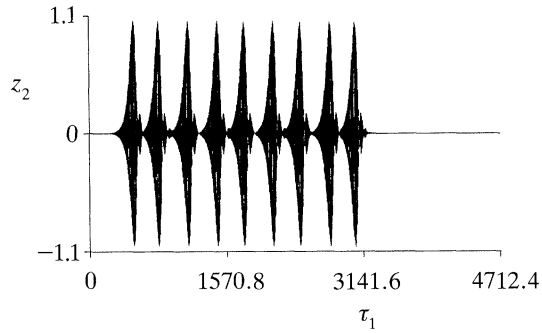

Figure 36. Time response of the out-of-plane component displaying transient chaos; $\alpha = 0.5$, $\beta = 4.49$, $\epsilon = 0.1$.

Figure 37

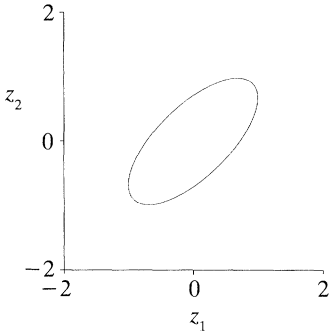

Figure 38

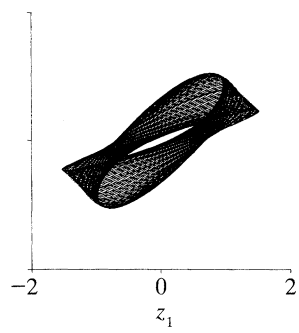

Figure 39

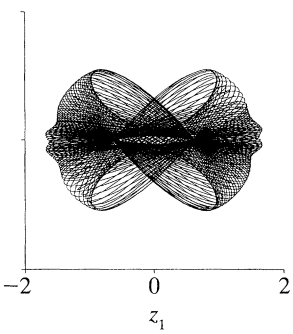

Figure 37. Periodic non-planar response of whirling motion of the string; $\alpha = 0.513$, $\beta = 2.4$, $\epsilon = 0.1$.

Figure 38. Non-symmetric almost periodic response of the string; $\alpha = 0.513$, $\beta = 3.0$, $\epsilon = 0.1$.

Figure 39. Symmetric almost periodic response of the string; $\alpha = 0.513$, $\beta = 3.3$, $\epsilon = 0.1$.

the lower planar fixed point. Figure 36 shows the corresponding time history of the non-planar component. This figure demonstrates the dramatic effect that a crisis has on the dynamics of the system.

(iii) *Physical interpretation of solutions*

Before closing this discussion, it may be of interest to visualize the physical motion of the string corresponding to the various attractors. Figures 37–39 show the response in the $z_{11}\, z_{12}$ plane for $\beta = 2.4$ and 3.3 respectively. This plane can be thought of as viewing along the axis of the string as it vibrates. At $\beta = 2.4$, the string undergoes a non-planar 2π-periodic motion which is the well-known whirling or ballooning motion of the string. Owing to a change in excitation frequency, this periodic motion becomes unstable and gives rise to the almost periodic motion in figure 38 for $\beta = 3.0$. The ballooning motion now precesses or drifts periodically at a slow rate, i.e. the spatial orientations as well as the magnitudes of the semi major and minor axes oscillate slowly in time. Note that the two motions are not symmetric about the plane of excitation and exist with their symmetric counterparts. A further change in the frequency of excitation can result in the collision of the two precessing motions to give the symmetric precessing motion of figure 39. This motion is the one which ultimately breaks down into chaos.

Figure 40

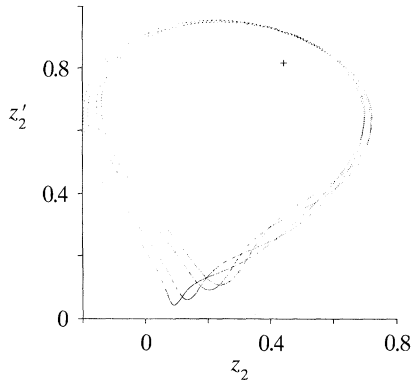

Figure 41

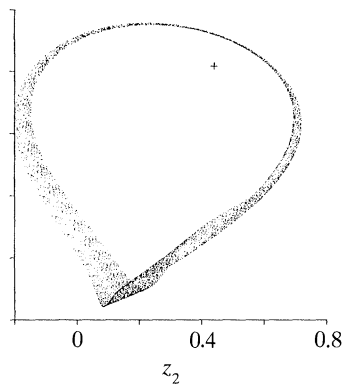

Figure 40. Poincaré section of the Rössler type T_4 solution; $\alpha = 0.513$, $\beta = 3.24$, $\epsilon = 0.025$.

Figure 41. Poincaré section of the Rössler type chaotic attractor; $\alpha = 0.513$, $\beta = 3.26$, $\epsilon = 0.025$.

(*e*) *Smaller values of* ϵ*: Rössler type chaos*

The previous subsections detailed some of the similarities and differences between the solutions of the averaged system and those of the non-autonomous system for a particular value of ϵ ($= 0.1$). One particularly striking difference was the absence of multiple torus-doubling bifurcations in the isolated branch before the merger of the symmetric twins and the creation of the larger symmetric torus. It is clear from earlier discussions that as $\hat{\epsilon}$ is reduced more torus-doubling bifurcations should be observed in this branch. This indeed is the case. Figure 40 shows a Poincaré section of the Rössler type T_4 solution for $\epsilon = 0.025$, $\beta = 3.24$, and $\alpha = 0.513$. Such solutions did not exist at $\epsilon = 0.1$. At $\epsilon = 0.025$ a Rössler type chaotic attractor is also found in the non-autonomous system. Figure 41 shows a Poincaré section of the Rössler type chaotic attractor for $\epsilon = 0.025$, $\beta = 3.26$, and $\alpha = 0.513$.

At this point, let us make a few remarks about keeping only one mode ($N = 1$) in (6) for the investigations with the truncated string equations. We first recall that the nonlinear coupling in the various modal amplitudes z_j is such that the modes not directly excited remain at rest if started with zero initial conditions. Thus, the four-dimensional submanifold of non-zero $(z_r, \dot{z}_r)$ is an integral manifold of the system and the dynamical behaviour presented in this section takes place on that manifold. If small initial conditions away from the integral manifold are given, their effects can be investigated by considering the non-autonomous modal amplitude equations (6) and this has been termed the problem of 'local stability of modes at rest' in the literature (Henry & Tobias 1961; Ariaratnam 1987; Hsieh & Shaw 1990). When the rth mode, which is the directly excited mode, undergoes periodic oscillations, the equations for inactive modes have periodic coefficients leading to the well-known Mathieu–Hill type equations. Linear stability can then be investigated using the standard Floquet theory and the so called 'strutt' diagrams. Since the natural frequencies and the parametric excitation are not in 'principal parametric resonance', one can easily show that even for small damping, the modes at rest are asymptotically stable. The situation is more complex when the active mode has almost periodic motion (Davis & Rosenblat 1980). For the case of chaotic motions of the active mode, no direct results regarding the stability of zero solutions of modes

at rest are available. The chaotic input can be perhaps treated as a stochastic signal with certain statistical properties and then concepts from the literature on 'almost-sure-stability' can be used to study the response properties. This is a very interesting area that needs to be investigated. Hsieh & Shaw (1990) have made some initial attempts in this direction.

6. Summary and conclusions

This work studied an N-mode truncation of the equations governing the resonantly forced nonlinear motions of a stretched string. The external forcing is restricted to a plane, and is harmonic with the frequency near a linear natural frequency of the string. The method of averaging is used to investigate the weakly nonlinear dynamics. Using the amplitude equations it is shown that to $O(\hat{\epsilon})$, only the resonantly forced mode has non-zero amplitude.

Steady-state solutions of the averaged equations are studied in considerable detail. Both planar (i.e. lying in the plane of forcing) and non-planar solutions are studied and amplitude–frequency curves are determined. For small enough damping, it is found that the solutions in the non-planar branch become unstable via a Hopf bifurcation. This branch of limit cycles exhibits several period-doubling bifurcations, but does not directly result in the formation of a chaotic attractor.

At lower values of damping, other branches of periodic solutions are discovered and explored. An isolated branch of periodic solutions is created at some frequency, via a saddle-node bifurcation. The genesis of this branch involves the simultaneous creation of a stable periodic solution branch and an unstable periodic solution branch. As damping is decreased further, these branches undergo various bifurcations. The unstable isolated branch eventually merges with the stable Hopf branch via a saddle-node bifurcation, whereas solutions in the stable isolated branch undergo a cascade of period-doubling bifurcations that results in the formation of a Rössler type chaotic attractor. It is discovered that as damping is reduced further, a series of isolated branches are created and merged into the extended Hopf branch. Each new isolated branch is found to have a period longer than the previously created branch. The process of isolated branch creation and merger culminates in the formation of a homoclinic orbit originating from a saddle-focus. The eigenvalue structure of the saddle-focus and Sil'nikov's theorem are used to interpret the bifurcation behaviour observed in numerical simulations. Away from the homoclinicity frequency, a series of bifurcations result in the formation of a Lorenz type chaotic attractor.

At still lower values of damping, an interval in frequency is discovered where the Lorenz type attractor abruptly disappears. This phenomena is explained through the concept of a boundary crisis. The crisis frequencies quickly approach the Hopf bifurcation frequencies as α is decreased. Even though the bifurcations take place over an increasingly small interval of frequency detuning β, the bifurcation sequence remains essentially unchanged.

The results from the investigations with the averaged system are interpreted for the truncated string system using results from the averaging theory. Extensive numerical investigations show that for the single-mode truncation of the non-autonomous system, there seems to be a correspondence even between chaotic solutions of the averaged system and those of the original system. Counterparts to

PHILOSOPHICAL TRANSACTIONS OF THE ROYAL SOCIETY A MATHEMATICAL, PHYSICAL & ENGINEERING SCIENCES

all phenomena found in the averaged system are found in the non-autonomous system.

Thus, the averaged equations provide a good explanation of experimental observations of previous investigators, including jump phenomena and non-planar whirling or ballooning. The averaged equations also predict the existence of stable motions of the string including almost periodic and aperiodic non-planar motions. A careful application of the method of averaging provides many insights into the behaviour of the non-autonomous system. The correspondence between the solutions of the averaged system and those of the non-autonomous system is quite good.

We would like to point out that there has been considerable recent interest in chaotic vibrations of strings. Latest works include the theses of Tufillaro (1990) and O'Reilly (1990). Although each of these, and the present work, consider the problem of forced vibrations of the string in the context of one-degree and two-degrees of freedom models, the methods used are markedly different. The work of O'Reilly (also see O'Reilly & Holmes 1991) is more closely related to the present study except that it uses techniques from global dynamics, and investigates the predicts the complexity of bifurcations and motions in terms of the completely integrable hamiltonian system obtained when the damping and the forcing tend to zero.

The authors thank Dr N. F. Tufillaro for the copy of his thesis, and Professor P. Holmes and Dr O. M. O'Reilly for copies of the preprints. The authors also thank the referees for thoughtful comments and suggestions that have improved the presentation.

References

Anand, G. V. 1966 Non-linear resonance in stretched strings with viscous damping. *J. acoust. Soc. Am.* **40**, 1517–1528.

Anand, G. V. 1973 Negative resistance mode of forced oscillations of a string. *J. acoust. Soc. Am.* **54**, 692–698.

Ariaratnam, S. T. 1987 Stochastic stability of modes at rest in coupled nonlinear systems. In *Nonlinear stochastic dynamic engineering systems* (ed. F. Ziegler & G. I. Schuheller). New York: Springer-Verlag.

Arneodo, A., Coullet, P. H. & Spiegel, E. A. 1983 Cascade of period doublings of tori. *Phys. Rev. Lett.* A **94**, 1–6.

Aronson, D. G., Chory, M. A., Hall, G. R. & McGeehee, R. P. 1982 Bifurcations from an invariant circle for two-parameter families of maps of the plane: a computer assisted study. *Communs math. Phys.* **83**, 303–354.

Bajaj, A. K. & Johnson, J. M. 1990 Asymptotic techniques and complex dynamics in weakly nonlinear forced mechanical systems. *Int. J. Nonlinear Mech.* **25**, 211–226.

Bajaj, A. K. & Tousi, S. 1990 Torus doublings and chaotic amplitude modulations in a two degree-of-freedom resonantly forced mechanical system. *Int. J. Nonlinear Mech.* **25**, 625–642.

Benettin, G., Galgani, L., Giorgilli, A. & Strelcyn, J. M. 1980 Lyapunov characteristic exponents for smooth dynamical systems and for Hamiltonian systems: a method for computing all of them. *Meccanica* **15**, 9–30.

Chenciner, A. & Iooss, G. 1979 Bifurcations de tores invariants. *Arch. ration. Mech. Analysis* **69**, 108–198.

Davis, S. H. & Rosenblat, S. 1980 A quasi-periodic Mathieu-Hill equation. *SIAM J. appl. Math.* **38**, 139–155.

Doedel, E. 1986 *AUTO: Software for continuation and bifurcation problems in ordinary differential equations*. Report, May 1986, Department of Applied Mathematics. California Institute of Technology.

Eller, A. I. 1972 Driven nonlinear oscillations of a string. *J. acoust. Soc. Am.* **51**, 960–966.

Farmer, J. D., Ott, E. & Yorke, J. A. 1983 The dimension of chaotic attractors. *Physica* D **7**, 153–180.

Frederickson, P., Kaplan, J. L., Yorke, E. D. & Yorke, J. A. 1983 The Liapunov dimension of strange attractors. *J. diff Equat.* **49**, 185–207.

Funakoshi, M. & Inoue, S. 1988 Surface waves due to resonant horizontal oscillation. *J. Fluid Mech.* **192**, 219–247.

Funakoshi, M. & Inoue, S. 1990 Bifurcations of limit cycles in surface waves due to resonant forcing. *Fluid Dyn. Res.* **5**, 255–271.

Glendinning, P. 1984 Bifurcations near homoclinic orbits with symmetry. *Phys. Lett.* A **103**, 163–166.

Glendinning, P. & Sparrow, C. 1984 Local and global behavior near homoclinic orbits. *J. statist. Phys.* **35**, 645–696.

Grebogi, C., Ott, E. & Yorke, J. A. 1983 Crises, sudden changes in chaotic attractors, and transient chaos. *Physica* D **7**, 181–200.

Guckenheimer, J. & Holmes, P. J. 1983 *Nonlinear oscillations, dynamical systems, and bifurcations of vector fields.* New York: Springer-Verlag.

Hale, J. K. 1963 *Oscillations in nonlinear systems.* New York: McGraw Hill.

Hale, J. K. 1969 *Ordinary differential equations.* New York: John Wiley.

Henry, R. F. & Tobias, S. A. 1961 Modes at rest and their stability in coupled nonlinear systems. *J. mech. Engng Sci.* **3**, 163–173.

Hsieh, S. R. & Shaw, S. W. 1990 The stability of modes at rest in a chaotic system. *J. Sound Vib.* **138**, 421–431.

Iooss, G. 1979 *Bifurcation of maps and applications.* Amsterdam: North-Holland.

Iooss, G. & Joseph, D. D. 1980 *Elementary stability and bifurcation theory.* New York: Springer-Verlag.

Johnson, J. M. 1989 On the vibration of stretched strings. Ph.D. dissertation, Purdue University, U.S.A.

Johnson, J. M. & Bajaj, A. K. 1989 Amplitude modulated and chaotic dynamics in resonant motion of strings. *J. Sound Vib.* **128**, 87–107.

Kaneko, K. 1984 Oscillation and doubling of torus. *Prog. Theor. Phys.* **72**, 202–215.

Kaplan, J. L. & Yorke, J. A. 1978 Functional differential equations and the approximation of fixed points. *Lect. Notes in Math.*, no. 730 (ed. H. O. Peitgen & H. O. Walther). Berlin: Springer-Verlag.

Keller, H. B. 1977 Numerical solution of bifurcation and nonlinear eigenvalue problems. In *Applications of bifurcation theory* (ed. P. H. Rabinowitz). New York: Academic Press.

Knobloch, E. & Weiss, N. O. 1983 Bifurcations in a model of magnetoconvection. *Physica* D **9**, 379–407.

Maewal, A. 1986 Chaos in a harmonically excited elastic beam. *ASME J. appl. Mech.* **53**, 625–632.

Maewal, A. 1987 Miles' evolution equations for axisymmetric shells: simple strange attractors in structural dynamics. *Int. J. Nonlinear Mech.* **21**, 433–438.

Mees, A. & Sparrow, C. 1987 Some tools for analyzing chaos. *Proc. Inst. elect. Electron. Engrs.* **75**, 1058–1070.

Miles, J. W. 1965 Stability of forced oscillations of a vibrating string. *J. acoust. Soc. Am.* **38**, 855–861.

Miles, J. W. 1984*a* Resonant, nonplanar motion of a stretched string. *J. acoust. Soc. Am.* **75**, 1505–1510.

Miles, J. W. 1984*b* Resonant motion of a spherical pendulum. *Physica* D **11**, 309–323.

Miles, J. W. 1984*c* Recently forced surface waves in a circular cylinder. *J. Fluid Mech.* **149**, 15–31.

Molteno, T. C. A. & Tufillaro, N. B. 1990 Torus doubling and chaotic string vibrations: experimental results. *J. Sound Vib.* **137**, 327–330.

Morse, P. M. & Ingard, V. 1968 *Theoretical acoustics.* New York: McGraw Hill.

Narasimha, R. 1968 Nonlinear vibration of an elastic string. *J. Sound Vib.* **8**, 134–146.

Nayfeh, A. H. & Mook, D. T. 1979 *Nonlinear oscillations.* New York: Wiley-Interscience.

PHILOSOPHICAL TRANSACTIONS OF THE ROYAL SOCIETY A MATHEMATICAL, PHYSICAL & ENGINEERING SCIENCES

O'Reilly, O. M. 1990 The chaotic vibration of a string. Ph.D. thesis, Cornell University, U.S.A.

O'Reilly, O. M. & Holmes, P. 1991 Nonlinear, nonplanar and nonperiodic vibrations of a string. *J. Sound Vib.* (In the press.)

Parker, T. S. & Chua, L. O. 1987 Chaos: a tutorial for engineers. *Proc. Inst. elect. Electron. Engrs* **75**, 982–1008.

Schapiro, S. M. & Sethna, P. R. 1977 An estimate of the small parameter in the asymptotic analysis of nonlinear systems by the method of averaging. *Int. J. Non-Linear Mech.* **12**, 127–140.

Sethna, P. R. & Bajaj, A. K. 1978 Bifurcations in dynamical systems with internal resonance. *ASME J. appl. Mech.* **45**, 895–902.

Sil'nikov, L. P. 1970 A contribution to the problem of the structure of an extended neighborhood of a rough equilibrium state of saddle-focus type. *Math. USSR Sbornik* **10**, 91–102.

Streit, D. A., Bajaj, A. K. & Krousgrill, C. M. 1988 Combination parametric resonance leading to periodic and chaotic response in two degree-of-freedom systems with quadratic nonlinearities. *J. Sound Vib.* **124**, 297–314.

Tousi, S. & Bajaj, A. K. 1985 Period-doubling bifurcations and modulated motions in forced mechanical systems. *ASME J. appl. Mech.* **52**, 446–452.

Tufillaro, N. B. 1989 Nonlinear and chaotic string vibrations. *Am. J. Phys.* **57**, 408–414.

Tufillaro, N. B. 1990 Chaotic themes from strings. Ph.D. Thesis, Bryn Mawr College, U.S.A.

Wiggins, S. 1988 *Global bifurcations and chaos.* New York: Springer-Verlag.

Wolf, A., Swift, J. B., Swinney, H. L. & Vastano, J. A. 1985 Determining Lyapunov exponents from a time series. *Physica* D **16**, 285–317.

Received 5 September 1990; revised 15 March 1991; accepted 28 June 1991

PHILOSOPHICAL TRANSACTIONS OF THE ROYAL SOCIETY A MATHEMATICAL, PHYSICAL & ENGINEERING SCIENCES